

## High sorption materials for SFL – A literature review

Lindsay Krall, Svensk Kärnbränslehantering AB

Maj 2012

**Svensk Kärnbränslehantering AB**

Swedish Nuclear Fuel  
and Waste Management Co

Box 250, SE-101 24 Stockholm  
Phone +46 8 459 84 00



ISSN 1402-3091

SKB R-12-10

ID 1343618

## **High sorption materials for SFL – A literature review**

Lindsay Krall, Svensk Kärnbränslehantering AB

Maj 2012

## Abstract

This literature survey is part of a project called the SFL Concept Study, carried out at SKB during the years 2011 to 2013, which investigates possible repository concepts for long-lived, low and intermediate level waste. The addition of a high sorption material has been proposed as a means through which releases may be limited from the near-field. In the previous repository concept from 1999 (SFL 3-5), the transport of cationic nuclides was expected to be reduced by their adsorption to the cement, gravel, and bedrock. However, in the preliminary safety assessment of that previous concept, it was found that the key radionuclides are mainly anions. Thus, this literature survey has placed special emphasis on the adsorption of anions. Due to their high release and dose rates from the far field, Cl-36, Mo-93, C-14, and I-129 were of particular interest.

Ion exchange and surface complexation are the main adsorption mechanisms. Ion exchange is theoretically reversible and involves the isomorphic substitution of either (a) cation(s) or anion(s) in a mineral structure. The ions exchanged do not need to have the same charge, but the exchange should be stoichiometric. Surface complexation is more dependent on pH, and the strength of the bond formed (and thus the reversibility of the reaction) is partially dependent on the type of complex formed. A material's adsorption mechanism and efficiency is a function of its structure and charge density, but it will also vary as a function of pH, the type and amount of competing ions, and the concentration of the solute in solution.

A substantial body of work exists that investigates the application of materials that can remediate groundwater through the adsorptive removal of the contaminant(s). Application of such a function in the future SFL repository will differ from remediation applications in that the system will be more complex and heterogeneous than most of the contaminated waters studied, the adsorption processes must be passive, and the material must be suitable over a much longer period of time. Bentonite and zeolite are the most relevant cation exchangers. While bentonite may be applicable, to develop a concept around zeolite may require a substantial work and resources. Moreover, the 1999 assessment results suggest that cation exchange is not necessarily a concern due to adsorption to concrete, gravel, and bedrock. Layered double hydroxides are a class of clays that have been investigated for their anion exchange capacities, which are high at pH below neutral. Hydrous metal oxides are amphoteric, which implies that they adsorb anions at low pH and cations at high pH. The exchange capacity and the pH demarking the transition from cation to anion exchange varies by type of oxide. Zero-valent iron (ZVI) and red mud are the most complex materials, which may imply versatility. ZVI in itself is not an adsorbent, but it will corrode if utilized. The corrosion products may be capable of adsorbing anions and cations, but the specific species and adsorption capacities will change over time as corrosion continues. Hematite would be the final corrosion product. Red mud, a highly alkaline waste product of bauxite processing, and its derivations are complex in that they are comprised of a variety of minerals. These include zeolite-like minerals that may adsorb cations, amphoteric metal oxides, and LDHs when neutralized with seawater.

Beyond its apparent versatility as an adsorbent, this survey also found investigations into the potential application of red mud to cement, building materials, and as an adsorbent in a shallow LLW repository. Since it is also available in large quantities and possibly less costly than ordinary Portland cement, basic studies comparing the properties of these two materials may be interesting and worthwhile. Still, further information regarding the site conditions and the disposal concept in general would be helpful in determining the most efficient adsorbent.

# Sammanfattning

Denna litteraturstudie är en del av projektet SFL Konceptstudie, vars syfte är att ta fram ett nytt koncept för slutförvar för långlivat låg- och medelaktivt avfall. Det nya konceptet ska erbjuda en förbättring vad gäller långsiktig säkerhet, jämfört med det tidigare konceptet SFL 3-5 vilket togs fram och analyserades år 1999. I SFL Konceptstudie har användning av material med hög sorptionsförmåga har föreslagits som metod för att begränsa utsläpp från närområdet. Här har särskild vikt lagts vid sorption av negativt laddade joner (anjoner). Baserat på resultatet av den tidigare säkerhetsanalysen av SFL 3-5, ligger fokus på de rörliga nukliderna Cl-36, Mo-93, C-14, och I-129.

Jonbyte och ytkomplexbildning är de mekanismer som är viktigast vid sorption. Jonbyte är, en reversibel process och innefattar substitution av antingen katjoner eller anjoner i en mineralstruktur. Bildning av ytkomplex är mer pH-beroende än jonbyte, och styrkan hos den bindning som bildas (och således möjligheten att reversera reaktionen) är delvis beroende av vilken komplextyp som bildas. Materialets struktur och laddningsdensitet påverkar vilken sorptionsmekanism som är aktiv och även dess effektivitet, men sorptionen varierar även som en funktion av pH, typen och mängden av konkurrerande joner, samt koncentrationen av det sorberande ämnet i vattenfasen.

Bentonit och zeolit är de mest relevanta materialen när det gäller katjonbyte. Det är möjligt att bentonit kan tillämpas, men att utveckla ett koncept kring zeolit kräver omfattande arbete och resurser. Dessutom tyder resultaten i den tidigare säkerhetsanalysen på att tillsättning av ett speciellt material för katjonbyte inte nödvändigtvis har högst prioritet, eftersom katjonerna sorberar relativt bra på betong, grus och berg (material som redan ingår i de flesta koncept). I stället ligger alltså fokus på att tillsätta ett material som kan sorbera anjoner; ett exempel är en typ av leror som kallas LDH (Layered Double Hydroxide). Olika LDH:er har undersökts för deras höga sorptionskapacitet för anjoner vid låga pH. Det finns också vattenhaltiga metalloxider som sorberar anjoner vid låga pH och katjoner vid höga pH; dessa kallas amfoter. Det pH-värde som markerar övergången från sorption av anjoner till sorption av katjoner beror på typ av oxid. Metalliskt järn (Zero Valent Iron, ZVI) och rödslam (restprodukt från aluminiumframställning) är komplexa och mångsidiga material. ZVI är i sig inte ett sorberande material, men vid korrosion i naturliga miljöer bildas det ett mineralogiskt komplext ytskikt. Korrosionsprodukterna i ytskiktet kan sorbera både anjoner och katjoner, men kapaciteten för olika typer av joner förändras under tiden som korrosionen pågår. Den slutliga korrosionsprodukten är i många fall hematit. Rödslam, en kraftigt alkalisk restprodukt av bauxitbearbetning, är ett mineralogiskt komplext material. Vilka mineral som ingår i rödslam beror på hur det bearbetas och prepareras, men bland annat ingår zeolit-liknande ämnen som kan sorbera katjoner, amfoter metalloxider och LDH:er.

Rödslam har potential inte bara som sorptionsmaterial i vattenreningssystem – det har för detta syfte studerats som möjligt material i ett förvar för lågaktivt radioaktivt avfall – utan även som ett slags cement eller byggnadsmaterial. Eftersom det finns tillgängligt i stora mängder och möjligen är billigare än vanlig Portland cement, kan grundläggande studier som jämför egenskaperna hos dessa två material vara intressant och givande. Kunskap om förhållandena på platsen och mer detaljerad information om konceptet i allmänhet behövs dock för att kunna avgöra vilket material som är mest lämpligt.

# Contents

<b>1</b>	<b>Introduction</b>	<b>7</b>
1.1	Background	7
1.2	Purpose and scope	7
<b>2</b>	<b>Method</b>	<b>9</b>
<b>3</b>	<b>Relevant Radionuclides</b>	<b>11</b>
3.1	Selection of Relevant Nuclides	11
3.2	Basic chemical characteristics of selected radionuclides	15
<b>4</b>	<b>Sorption background</b>	<b>17</b>
4.1	Sorption mechanisms	17
4.2	Terms and parameters influencing sorption efficiency	18
<b>5</b>	<b>Materials</b>	<b>23</b>
5.1	Barrier Concepts and List of Barrier Materials	23
5.2	Bentonite	24
5.3	Zeolite	24
5.4	Layered Double Hydroxide (LDHs)	27
5.5	Hydrous metal oxide (amphoteric)	29
5.6	Red Mud	32
5.6.1	Untreated red mud	32
5.6.2	Acid-treated red mud	34
5.6.3	Seawater-treated red mud	34
5.6.4	Applied to nuclear waste disposal	35
5.7	Zero-valent iron (ZVI) and corrosion products	37
<b>6</b>	<b>Discussion</b>	<b>39</b>
<b>7</b>	<b>Conclusions</b>	<b>43</b>
	<b>References</b>	<b>45</b>

## Abbreviations

AEC	Anion exchange capacity
BET	Adsorption theory by S Brunauer, PH Emmett, E Teller
CEC	Cation exchange capacity
IEP	Isoelectric Point
KBS-3	Technology for disposal of high-level radioactive waste
$K_d$ (m <sup>3</sup> /kg)	Linear distribution coefficient
LDH	Layered double hydroxide
PRB	Permeable reactive barrier
PSA	Preliminary Safety Assessment
PZC	Point-of-zero charge
PZNPC	Point-of-zero-net-proton-charge
$R_a$	Acid-treated red mud
$R_{ah}$	Acid- and heat-treated red mud
$R_w$	Water-treated red mud
SFL	Final repository for long-lived low- and intermediate-level waste
SFR	Final repository for short-lived low- and intermediate-level waste
SKI	Swedish Quality Index
ZVI	Zero-valent iron

# 1 Introduction

## 1.1 Background

In 1999, SKB reported the results of a Preliminary Safety Assessment (PSA) of SFL 3-5 (SKB 1999). This was done to evaluate the repository concept for long-lived low- and intermediate-level waste as it was envisaged during that time. At the present time of writing, SKB is investigating other repository concepts for this type of waste in a project called SFL Concept study, which will run until 2013. The goal of that study is to propose one, or a maximum of two, repository concepts which will be further evaluated using an updated inventory and a relevant safety assessment methodology.

The SFL 3-5 concept of 1999 envisioned safety functions of steel and concrete waste packages to limit diffusivity and a crushed rock backfill to create a hydraulic cage. The concrete and crushed rock would also function as sorptive barriers to the escape of radionuclides. In the international review of the SFL 3-5 assessment, published by SKI in 2000 (Chapman et al. 2000), it was observed that small changes in the sorption of key radionuclides had a large effect on released dose rates. This should be the object of further investigations.

In 2011, the SFL Concept study identified a number of concepts which will be further evaluated. The concepts are focused on different types of barrier materials (cement, bentonite, gravel) which will provide different functions that contribute to safety. In addition, different waste conditioning and barrier-improving options were suggested for evaluation. One of these options is called “High sorption”, which suggests the addition of large amount of some material which can stabilize the waste through, among other processes, sorption to significantly reduce down the near-field release. The “High sorption” option is non-specific with regards to which type of material should be used. In order to evaluate the possibilities to use such a material, more information is needed regarding key radionuclides and available relevant materials.

## 1.2 Purpose and scope

The purpose of this report is to provide a review of existing information on materials with relevant sorptive properties for possible consideration during the development of new SFL concepts. Different mechanisms and processes have been identified by which materials added to the SFL repository may delay the release of radionuclides in the near field. These include:

1. Formation of a stable chemical compound.
2. Chemisorption on active surfaces.
3. Physisorption.
4. Trapping of select molecules that complement a porous material in terms of size and polarity.

In addition, pH and redox will affect these mechanisms and any material that may help to control the chemical environment may be important for the function of the materials in the long term.

The present report is focused primarily on materials which function by means of chemisorption, though certain materials, such as zeolites, can reduce contaminant mobility by both chemisorption and trapping. Articles describing results from physisorption experiments were scarce, and thus this mechanism receives little attention in this report. Furthermore, this report does not give significant consideration to precipitation (i.e. formation of a stable chemical compound). While this is another surficial process that could retard the release of radionuclides, more detailed data, such as thermodynamic inputs and interactions, would be required to draw justifiable inferences.

This report also contains a basic description of the chemical characteristics of the selected radionuclides and speculation as to the most attractive material(s) for their adsorptive containment based on characteristics such as structural integrity, chemical compatibility, and economic feasibility.

The sorptive properties of main barrier materials already considered (cement, bentonite) are being carefully evaluated elsewhere, and in the present report a brief description of bentonite is provided as reference and for comparison.

## 2 Method

The research behind this work largely consisted of searching for ‘sorption’-related terms in encyclopaedias available at the KTH and Karolinska libraries in Stockholm and in ScienceDirect and the ISI Web of Knowledge databases. Such resulted primarily in articles related to chemisorption, and thus this mechanism receives more attention than physisorption in this report.



## 3 Relevant Radionuclides

### 3.1 Selection of Relevant Nuclides

Figures 3-1, 3-2, and 3-3, show the radionuclide release rates that have resulted from the release and transport calculations described in detail in SFL Preliminary Safety Assessment (SKB 1999). The 1999 assessment involved a repository concept constructed of three parts: SFL 3, 4 and 5, containing different types of waste, and the hypothetical locations Aberg, Beberg and Ceberg, which had different site-specific characteristics. While the assumptions behind the calculations and the exact times of maximum release and maximum activity can be found in Section 8 of that report, Figures 3-1, 3-2, and 3-3 show the nuclides whose release rates should be reduced and thus candidates in considering materials for high sorption.

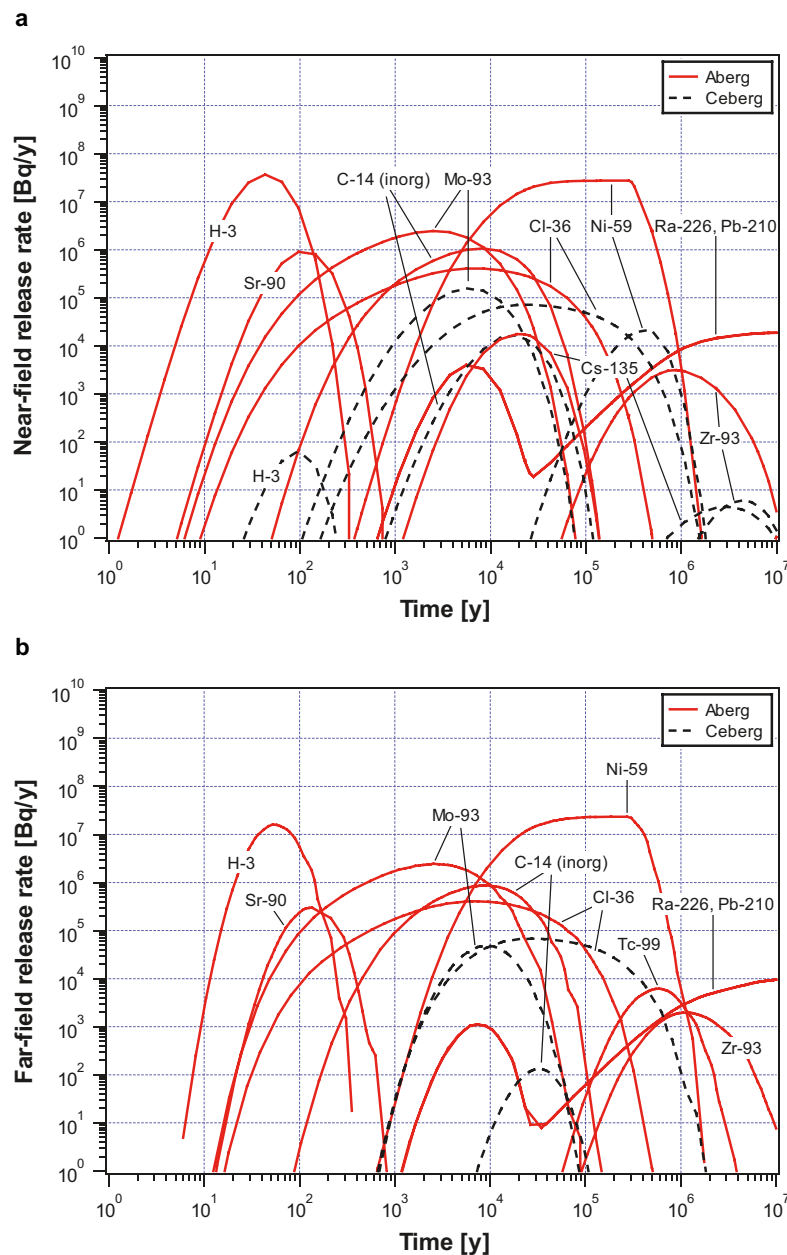


**Figure 3-1.** Radionuclide release rates from SFL 3 from (a) the near field and (b) the far field at Aberg and Ceberg for the basic calculation case within the reference scenario (Beberg, with intermediate release rates, is not included in the figure).

Differences between near and far field safety assessment results can be attributed to the influence of site-specific factors, such as water flow rate and composition, on the mobility of and thus the dose rates from individual nuclides. Water flow rate affects the advective travel time of the released nuclides from the near field to the far field. Water salinity can promote or decrease the adsorption onto or diffusion (matrix diffusion) into the bedrock of certain radionuclides. The scenario at Aberg is one of a high water flow rate (10 L/(m<sup>2</sup> year)) and saline groundwater. Beberg scenarios have a medium water flow rate (1 L/(m<sup>2</sup> year)) and both saline and non-saline groundwater. The flow-wetted surface area is also one order of magnitude larger than that in Aberg, allowing more opportunity for interaction between the nuclides and the bedrock matrix. Ceberg has a water flow rate of 0.1 L/(m<sup>2</sup> year), non-saline groundwater, and a flow-wetted surface area of the same order of magnitude as Aberg. Additionally, the penetration depth in the rock matrix is ten times that at Aberg and Beberg, which could be of importance for non-sorbing and low-sorbing nuclides. Nuclide release rates from the near-field models of each site are used as inputs for the respective far-field model. The mobility of the individual nuclides in the geosphere, described in Table 3-1, will determine the time of maximum release rate and the maximum release rate from the far field.

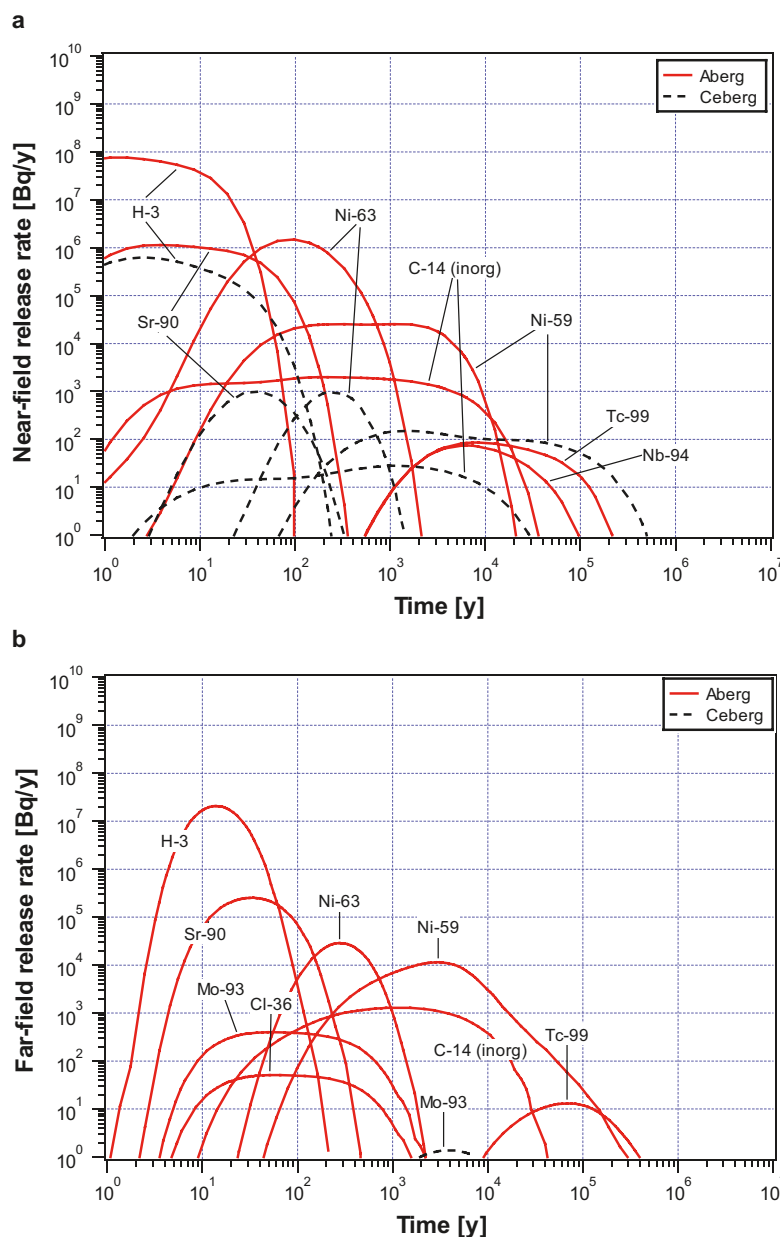


**Figure 3-2.** Radionuclide release rates from SFL 4 from (a) the near field and (b) the far field at Aberg and Ceberg (reference scenario and case without CRUD i.e. surface deposits are removed).

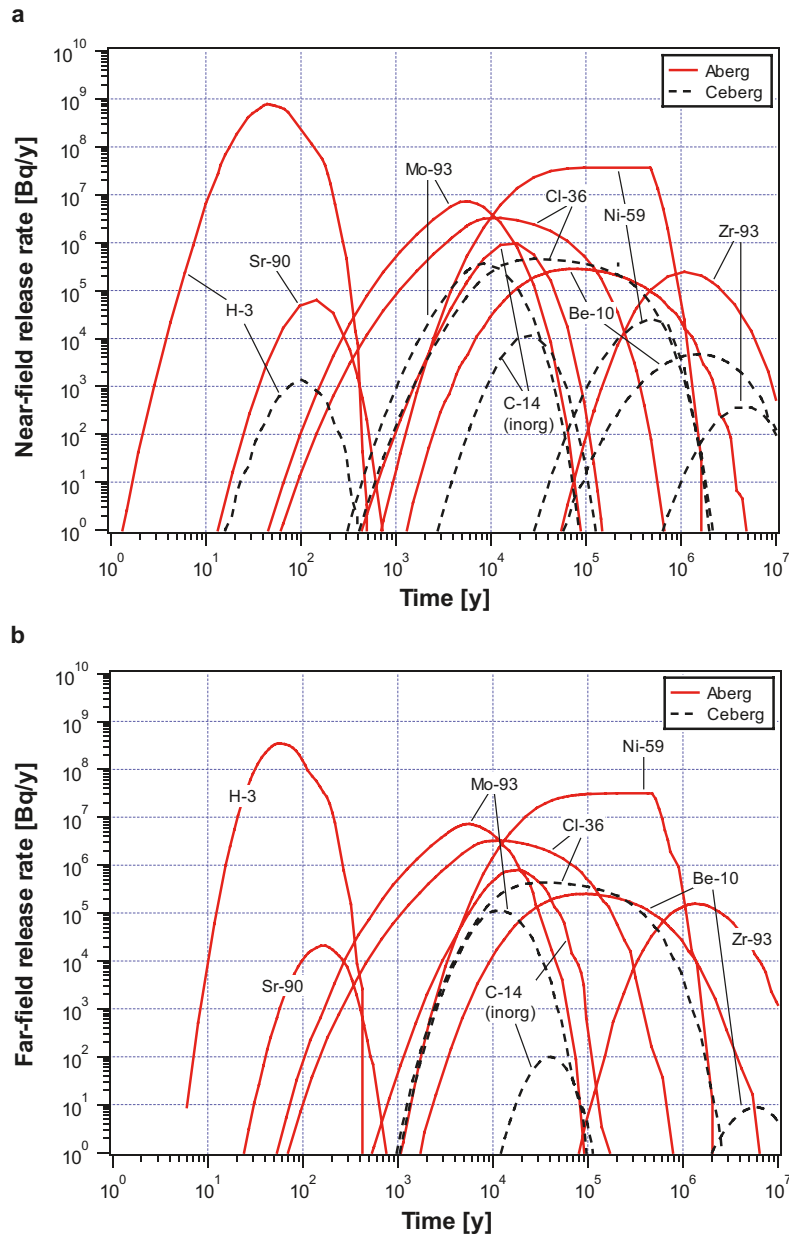


**Figure 3-3.** Radionuclide release rates from SFL 5 from (a) the near field and (b) the far field at Aberg and Ceberg (reference scenario).

**Table 3-1. Nuclides showing high release rates from the near and/or far field and description of transportation through geosphere, maximum release rate, and time of maximum release.**

Nuclide	Mobility and dose rate
H-3	Highest dose, but short half-life allows it time to decay if the advective travel time is longer, making it less important after $\sim 10^2$ years.
Be-10	Higher sorption in non-saline conditions, lower release rate. Long half-life, high dose to SFL 5 far field after $10^5$ years.
C-14 <sub>inorg</sub>	Decreased matrix diffusion in non-saline conditions, higher release rate; a dominant nuclide released from SFL 3 and SFL 5 in the near field, but has a short half-life, reducing the far field dose rate relative to the nuclides with longer half-lives.
Cl-36	Decreased matrix diffusion in non-saline conditions; higher release rate.
Co-60	Higher sorption in non-saline conditions; lower release rate.
Cs-135	Higher sorption & higher diffusion in non-saline conditions; lower release rate.
Cs-137	Higher sorption & higher diffusion in non-saline conditions; lower release rate.
I-129	Decreased matrix diffusion in non-saline conditions; higher release rate; long half-life.
Mo-93	Dominates far field release from SFL 3 and SFL 5 between $\sim 10^{2-3}$ and $10^{4-5}$ years.
Ni-59	Higher sorption in non-saline conditions; reduces maximum release from SFL 3 and SFL 5 at $10^5$ and $10^6$ years from repository closure. In non-saline water, maximum release rate is reduced by a factor of 400.
Ni-63	Higher sorption in non-saline conditions; lower release rate; SFL 4 at Aberg $\sim 10^2$ and $10^3$ years.
Pb-210	Higher sorption in non-saline conditions; lower release rate; SFL 3 $> 10^6$ years.
Ra-226	Higher sorption in non-saline conditions; lower release rate; SFL 3 $> 10^6$ years.
Se-79	Release rate relatively low. Still, max dose to Beberg (agricultural land) and Ceberg (peatland) less than only Cl-36 and Mo-93, but only after $10^5$ years SFL 3 and SFL 5.
Sr-90	Higher sorption & higher diffusion in non-saline conditions; lower release rate; short half-life, peaks slightly after H-3 but dose rate 4 orders of magnitude lower than that of H-3.
Tc-99	From SFL 3 at Aberg when time $> 10^5$ years (release rate = $6 \times 10^3$ Bq/yr, $\sim 4$ orders of magnitude less than Ni-59).
Zr-93	Long half-life; high release rate in far field of SFL 3 and SFL 5 after $10^6$ years.

Cl-36 and Mo-93 are non-sorbing and long-lived, and dominate release rates between  $\sim 10^2$ – $10^3$  and  $10^4$ – $10^6$  years from SFL 3 and SFL 5 at each of the three sites. C-14 has a relatively short half-life and decays substantially by the time it reaches the far field in some scenarios. However, since 1999, the year in which the PSA was performed, there have been changes in the SFL reference inventory so C-14 release rates to the near and far fields may be higher than expected. I-129, Cl-36, Mo-93, and C-14 form anions and are thus highly mobile in the rock, though I-129 has much lower maximum release rates than Cl-36 and Mo-93.

Ni-59 and Ni-63 dominate nuclide release in a longer-term perspective ( $10^4$ – $10^6$  years), at which point any engineered adsorption barriers will, most likely, have degraded. Thus, bedrock in a non-saline environment may more effectively promote Ni-59 and Ni-63 adsorption than engineered barrier materials. In the short-term perspective (before  $10^2$  years), the short-lived H-3 and Sr-90 nuclides dominate release rates from each SFL 3, 4, and 5 at the Aberg site, where the water flow rate is relatively high. However, where the water flow rate is lower, i.e. at Ceberg, release rates from H-3 and Sr-90 are substantially reduced, particularly from the far-field, as the nuclides decay during the longer transport times. During the time period up to 10,000 years, release rates from Cl-36, Mo-93, and C-14 are high from SFL 3 and 5 under each site scenario (SKB 1999). These nuclides are long-lived and do not adsorb to cement, gravel, or bedrock. While the above figures do not indicate it to contribute a high release rate, I-129 has similar chemical properties to these nuclides and is a common constituent of radioactive waste in a broader sense. Thus, this report and the supporting research have emphasized materials that may adsorb the anions **Cl-36, Mo-93, C-14, and I-129**.

### 3.2 Basic chemical characteristics of selected radionuclides

The chemical characteristics and thus sorptive properties of the nuclides Cl-36, Mo-93, C-14, and I-129 depend on the natural conditions at the selected site and the conditions that will arise as the engineered barriers degrade. Site conditions should be reducing (low Eh) so as to limit the solubility of some nuclides in the waste and the corrosion rates of steel and iron barrier materials. The Aberg, Beberg, and Ceberg sites have reference Eh conditions of  $-0.308$ ,  $-0.250$ , and  $-0.202$  V, respectively. Alkaline conditions ( $\text{pH} = 12.5$ ) would be induced in the near field due to the degradation of concrete (a material which will probably be present irrespective of concept) and the introduction of large quantities of carbonate and hydroxide to the system. Saline waters reduce the effects of anion exclusion from microfissures in the bedrock. Thus, matrix diffusion should reduce anion transport in saline waters (SKB 1999).

In reducing conditions, Cl-36, C-14, and Mo-93 predominantly exist in solution as anionic species. C-14 is present in solution as carbonate species. As shown in Figure 3-4a, the prevailing species will be either  $\text{HCO}_3^-$  or  $\text{CO}_3^{2-}$  in the conditions relevant to the site. Mo-93, a transition metal, forms an oxyanionic species in the relevant site conditions (Figure 3-4b). Cl-36 and I-129 will be in the form of  $\text{Cl}^-$  and  $\text{I}^-$ , respectively, across the full range of pHs, except in very oxidizing Eh conditions, as shown in Figures 3-4c and 3-4d.

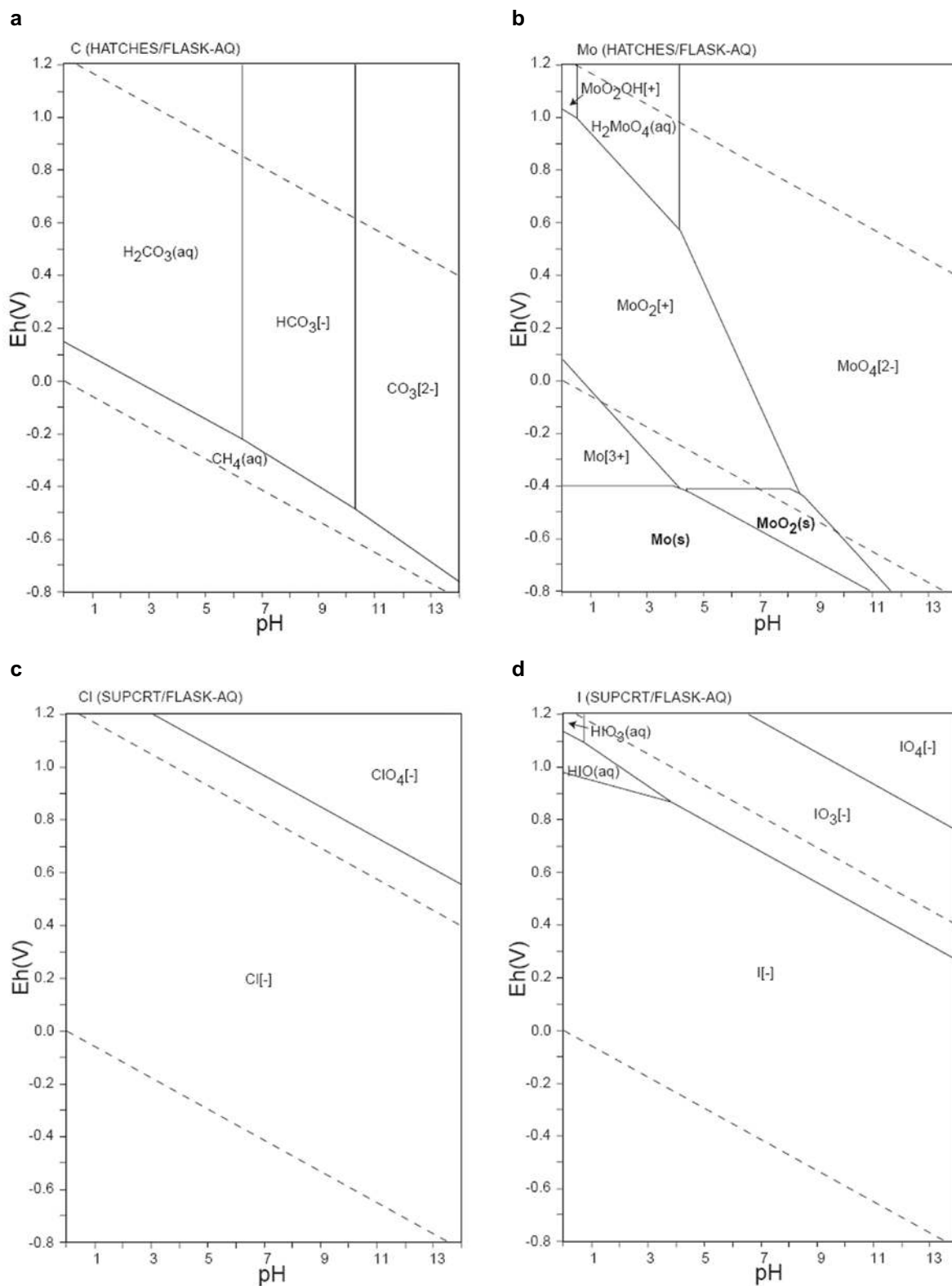


**Figure 3-4.** Eh-pH diagrams showing speciation of (a) C-14, (b) Mo-93, (c) Cl-36, and (d) I-129 across the range of natural Eh and pHs. From Geological Survey of Japan (2005).

## 4 Sorption background

### 4.1 Sorption mechanisms

An adsorption or desorption reaction is essentially a chemical reaction that occurs on a mineral or material surface, and thus it is driven by thermodynamics, or the free energy, heat content, entropy, and composition of the surface and interface. Ions adsorb to materials that have either a positive or negative net surface charge. This charge arises because of 1) isomorphic substitution of a cation of a similar radii but different charge into the structure of a crystal during its formation, and/or 2) reactions involving functional groups on the mineral surface and ions in solution. The charge due to ion substitution is considered a fixed charge, whereas the charge due to surface complexation is variable and dependent on the pH of the solution (Eby 2004). The major sorption mechanisms involving inorganic materials are considered to be ion exchange and surface complexation (Crawford 2010).

Ion exchange is considered to involve a purely electrostatic process. Either anions or cations can be exchanged, and though the valence and number of moles exchanged can differ, the exchange must be stoichiometric. Equation 4-1 demonstrates this exchange as applied to simple binary exchange (only two ionic species are involved in the exchange):



A and B are ionic species, a and b are the number of moles of each species, y and z are the electric charges of each species, and X is the solid phase involved in the ion-exchange process (Eby 2004). In principle, these processes are reversible, and the extent to which an exchanger can take up ions is called its 'capacity' (Dyer 2000).

The materials discussed with respect to surface complexation in this report are comprised of oxide and hydrous oxide minerals. In most conditions, functional groups ( $-\text{OH}$ ,  $-\text{COOH}$ ,  $-\text{OPO}_3\text{H}_2$ ,  $-\text{SH}$ ) are bound to the outer layer of the oxide surface at the sites of the under-coordinated metal ions (e.g.  $\text{Si}^{4+}$ ,  $\text{Al}^{3+}$ ,  $\text{Fe}^{3+}$ ) of the solid in an attempt to complete their coordination sphere. In the presence of water, hydroxyl ( $-\text{OH}$ ) is the dominant functional group bound to the surface (Tombácz 2002). As hydroxyl groups were the dominant surface functional group encountered in the literature survey and will be relevant to the repository site conditions, these will be the focus of the surface complexation reaction description, where surface charge varies as a function of pH. When the pH increases,  $\text{H}^+$  ions will leave the surface OH groups to form  $\text{H}_2\text{O}$  with the excess  $\text{OH}^-$  in solution and result in a negatively charged surface. The reverse occurs when the pH decreases. The *point of zero charge*, or the pH at which the surface charge is zero,  $\text{pH}_{\text{pzc}}$ , is also relevant to this type of sorption. As the solution pH decreases relative to the  $\text{pH}_{\text{pzc}}$ , more positive charges arise at surface and anion adsorption increases, while as the solution pH increases relative to the  $\text{pH}_{\text{pzc}}$ , cation adsorption increases (Eby 2004).

By definition, a substance that can act as either an acid or a base (that is, it reacts with a base or an acid, respectively), is termed 'amphoteric' (Wulfsberg 1987). Therefore, the materials described above are amphoteric, and they are of interest in this report because they can adsorb cations above the  $\text{pH}_{\text{pzc}}$  and anions below the  $\text{pH}_{\text{pzc}}$ . The  $\text{pH}_{\text{pzc}}$  varies between materials and will be addressed in the body of the report.

The surface complexation description becomes complicated because the mechanism involves both *inner sphere* and *outer sphere* surface complexes (Crawford 2010). *Outer sphere* adsorption complexes occur when a charged complex retains its hydration water and is hydrogen bonded or attracted to a surface through electrostatic forces. The process shares characteristics with ion exchange, but it is not necessarily due to permanent charges arising from isomorphous substitution nor are ions necessarily exchanged. *Inner sphere* adsorption complexes occur through loss of hydration water and the direct, short-range covalent bonding of the anionic or cationic complex to surface hydrogen or oxygen. In the case of positively-charged species, the bonding can be monodentate, bidentate, or multidentate or in the case of monovalent anions or oxyanions, the bonding can be mononuclear or binuclear, respectively (Parks 1990). Possible coordination and ion pairs formed in surface complexation are illustrated in Figure 4-1.



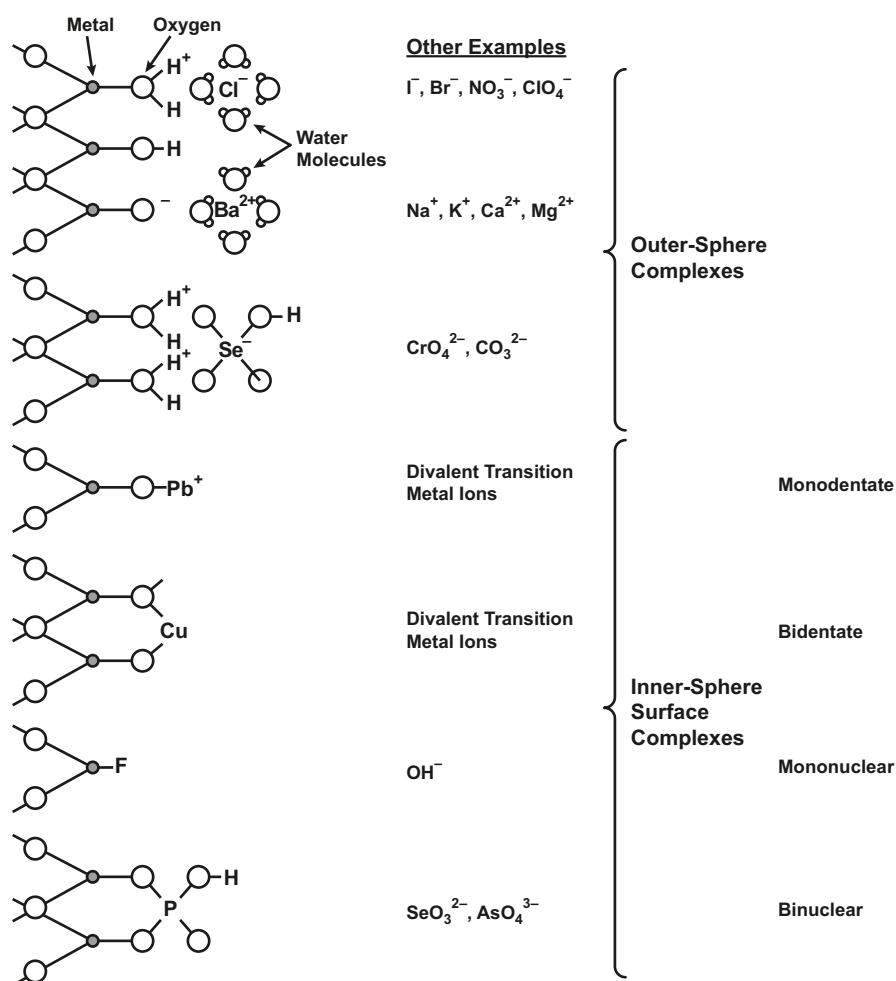


**Figure 4-1.** Schematic representation of surface complexes and ion pairs formed between hydroxyl groups of an oxide surface and inorganic ions. Adapted from Davis and Kent (1990).

## 4.2 Terms and parameters influencing sorption efficiency

The partitioning of species between solutions and particles is a chemically and physically complex process that depends on parameters similar to those involved in many types of chemical reactions. Below is a guide to the terms and concepts that will be discussed in the body of the report.

### *Coordinative surface charge*

Charge associated with the reactions of ions that determine electrical potential with surface functional groups. For oxides, which include both the adsorption of  $\text{H}^+$  or  $\text{OH}^-$  by the surface, but also coordination reactions of other ions with surface functional groups. Isoelectric point (IEP) is comprised of the point-of-zero-net-proton charge (PZNPC) and the point-of-zero charge (PZC) coordinative complex surface charge.

- $\text{pH}_{\text{pzc}}$ —the pH at which the sum of the charges of all adsorbed ions is zero,
- $\text{pH}_{\text{pznpc}}$ —the pH at which the charge due to the binding and release of protons and hydroxide ions is zero; differs from the pzc in that it accounts only for charges due to binding or release of  $\text{H}^+$  from the surface,
- $\text{pH}_{\text{IEP}}$ —the pH at which a particle carries no net electrical charge and the electrophoretic mobility is zero; equals the  $\text{pH}_{\text{PZNPC}}$  in oxide systems in which  $\text{H}^+$  and  $\text{OH}^-$  are the only potential-determining ions.

Surface coordination reactions of strongly adsorbing ions may shift the  $\text{pH}_{\text{PZNPC}}$  of an oxide to a new value because the adsorption of  $\text{H}^+$  is influenced by the adsorption of cations and the adsorption of  $\text{OH}^-$  by anions (Davis and Kent 1990).



### *Zeta potential*

Corresponds to the electrical charge at the effective shear (or slipping) plane, or the plane between the water molecules that are in the electrical field of the surface and move with the particle, and the stationary bulk water. The Zeta potential indicates the degree of repulsion between adjacent, similarly-charged particles in a dispersion. When the zeta potential is high (either negative or positive), the colloids are electrically stabilized, while when low (i.e. at or around the isoelectric point), the colloids will coagulate or flocculate (Davis and Kent 1990).

### *Cation-/Anion-Exchange Capacity (CEC/AEC)*

The amount of cations or anions that a mineral can accommodate on its respectively negatively or positively charged surface. It is typically expressed in terms of charge equivalents per unit mass (cmol/kg or meq/g). A charge equivalent is equal to one mole of ionic charge, or  $6.02 \times 10^{23}$  ion-exchange sites. Depending on the sorption mechanism, this can be permanent or variable (Crawford 2010).

### *Adsorption isotherm*

CEC/AEC denotes the overall ability of a material to adsorb ions while the isotherm, empirically determined, incorporates multiple variables that are involved in adsorption to describe the partitioning of a particular ion (Eby 2004). There are different approaches that are used, described by Crawford (2010) and listed below:

- $K_d$ —linear distribution coefficient approach, the simplest isotherm based method for modelling sorption being the ratio of immobilized and dissolved solute for a fixed solid phase composition, water chemistry, and solute concentration, typically given in  $m^3/kg$ . It does not account for mechanism or speciation and only applicable under exact conditions in which it is measured. It is not a physically accurate modelling approach, but most widely used in far-field transport problems, sorption independent of the concentration of the substance in solution. Defined in terms of the sorbed concentration,  $S$  (mol/kg) and aqueous phase concentration,  $C$  (mol/ $m^3$ ):

$$S = K_d C \quad (4-2)$$

- Freundlich isotherm, like  $K_d$ , is linear and assumes an unlimited number of unreacted surface sorbent sites:

$$C_{ads} = K C_{soln}^n \quad (4-3)$$

where  $K$  and  $n$  are constants for a given adsorbate and adsorbent, respectively, at a particular temperature.

- Langmuir isotherm, takes into account the finite nature of the number of sorbent sites:

$$C_{ads} = (S_{max} K C_{soln}) / (1 + K C_{soln}) \quad (4-4)$$

where  $S_{max}$  is the maximum sorptive capacity for the surface (i.e. the number of adsorption sites available per unit surface area).

- Langmuir-Freundlich isotherm, more recently developed analytical isotherm model that can be used to simulate pH-dependent adsorption:

$$q = \frac{Q_m (K_a C_{eq})^n}{(K_a C_{eq})^n + 1} \quad (4-5)$$

Where  $q$  is the amount of adsorbate adsorbed at equilibrium,  $Q_m$  is the adsorption capacity of the system,  $C_{eq}$  is the aqueous phase concentration at equilibrium,  $K_a$  is the affinity constant for adsorption, and  $n$  is the index of heterogeneity (Jeppu and Clement 2012).

These isotherms describe experimental data, and thus articles found during this literature survey typically reported the experiment results in these terms. However, empirical approaches to describing adsorption equilibria are considered unsatisfactory by many scientists because they fail to consider the overall aqueous geochemistry on which sorption relationships depend (Davis and Kent 1990). In spite of these shortcomings, these isotherm models do enable workers to compare the adsorption capabilities of different adsorbents (Santona et al. 2006).

#### *Surface Complexation Theory*

Describes adsorption in terms of chemical reactions between surface functional groups and dissolved chemical species, and thus is more appropriate and has been adopted for use in computer models. Extremely successful in simulating simple mineral-water systems, but more difficult to apply the modelling approach to natural systems. An important prerequisite for applying surface complexation theory is a detailed knowledge of surface functional groups, surface area, and the porosity of adsorbing mineral phases (Davis and Kent 1990).

#### *Surface Area, $S_{BET}$*

The surface area of a mineral is commonly measured using the BET method. The  $S_{BET}$  surface area specifies that the BET method has been used to determine the surface area.  $S_{BET}$  is an important predictor of ion exchange capacity when the charge on the material is fixed and is an important parameter in analyzing adsorption to bentonite and zeolite materials. However, where surface complexation is the predominant sorption mechanism, pH is a stronger indicator of adsorption efficiency than is  $S_{BET}$  (Crawford 2010).

#### *c-lattice parameter (length of interlayer region)*

The c-lattice parameter is relevant when a material, such as clays (i.e. bentonite or LDH, an anionic clay) adsorbs or intercalates an ion between its layers. The ion exchange would reach a maximum when the lattice is large enough for the ions to fit into the region for exchange. Thus, the ionic radius of the ion or nuclide is also a relevant parameter (Goh et al. 2008).

#### *Ionic strength/competition*

Ionic strength affects sorption directly and indirectly, depending on solute and its sorption characteristics. The most intuitive factor involves competition by groundwater components (e.g.  $\text{Ca}^{2+}$ ,  $\text{Mg}^{2+}$ ,  $\text{Na}^+$ ,  $\text{K}^+$ ,  $\text{CO}_3^{2-}$ ,  $\text{OH}^-$ ,  $\text{SO}_4^{2-}$ ,  $\text{Cl}^-$ , etc.) for ion exchange and surface complexation sites. Other factors that affect sorption reactions are related to surface charge and electrostatic effects (Crawford 2010). Specific adsorption of inorganic ions to the surface can change the value of the isoelectric point and affect the zeta potential of the dispersion (Davis and Kent 1990).

#### *pH and $[\text{CO}_3^{2-}]$*

The pH and carbonate contentiation of a solution influence chemical speciation, both of ions in solution and at mineral surfaces. Additionally, an anion exchanger can adsorb  $\text{OH}^-/\text{CO}_3^{2-}$  and a cation exchanger can adsorb  $\text{H}^+$  before or rather than the nuclides in solution (Crawford 2010).

#### *Temperature*

Temperature influences sorption because it influences the Gibbs free energy of a chemical reaction. In theory, solutes that have exothermic sorption reactions would be expected to show reduced sorptivity at higher temperatures, while solutes with endothermic reactions should show increased sorptivity. Theoretical analyses for monovalent ions by Sahai (2000) using *ab-initio* modelling techniques suggest that cation surface complexation reactions should increase modestly with temperature for most oxides, where anion surface complexation is predicted to decrease (Crawford 2010 and references therein). Regarding the nature of the reaction of oxyanions with LDHs (Section 5.4), some observations suggest that the process is exothermic, although a number of studies interpret the process to be endothermic. Still, others have reported an insignificant influence of temperature on the oxyanion adsorption by LDHs (Goh et al. 2008).

### *Redox conditions*

Redox conditions in the groundwater will influence valence state and therefore nuclide speciation (Crawford 2010). In addition, the basic structure and composition and thus sorption properties of the materials that consist of a large proportion of transition metals will also be affected by the redox conditions. Of the materials considered in this review, redox processes will have the most significant influence on zero-valent iron.

### *Selectivity*

Certain ions or ionic complexes are favoured to adsorb to an adsorbent over other species present in a solution. The order in which species are favoured, or the selectivity series, varies as a function of the physical and chemical properties of the material of interest; the valence state, ionic potential, and size of the hydration sphere of the cation or anion; and the coordination of the oxyanion. These parameters will affect physical properties related to electrostatic force and geometry of the ion and correspondingly the chemical interactions with at the interface (Crawford 2010). Ideally, an adsorbent will select for the nuclides determined to be critical, but complex interactions may interfere with this possibility.

## 5 Materials

### 5.1 Barrier Concepts and List of Barrier Materials

Research on barrier materials has predominantly catered to the environmental remediation sector, for instance to contain or decontaminate groundwater plumes. The Permeable Reactive Barrier (PRB) concept was developed to retard the flow of contaminant plumes, including those consisting of radionuclides that have been breached from inadequate waste storage at sites such as Hanford, WA and Mortandad Canyon, NM. Mixed wastes may require a multi-layer PRB. The barrier(s) are configured to suit the requirements of a specific site and its contaminants, and the materials used must be effective, inexpensive, and readily available in multiple-ton quantities. Impermeable barriers can be combined with the PRB to control the hydrological nature of the treatment zone (Conca et al. 2002).

While many of the characteristics discussed above are reminiscent of the multi-barrier concept integral to the design of a geological repository for radioactive waste, such an application requires additional considerations. Section 2.2 of the SR-Site main report (SKB 2011) provides an overview of the safety function of the barriers relevant to the final repository for spent fuel:

- The primary safety function of the barriers is to contain the fuel within a canister.
- Should containment be breached, the secondary safety function of the barriers is to retard a potential release from the repository.
- Engineered barriers shall be made of naturally occurring materials that are stable in the long term in the repository environment.

While the containment requirement (first bullet) is critical to the design of the spent fuel repository, the concept for the SFL repository for long-lived low- and intermediate-level waste will need to place greater emphasis on retardation of the release of radionuclides. Thus, sorption is an important process to consider in most suggested SFL concepts.

Materials that have been investigated and published for their sorptive properties are listed below. Some, such as bentonite, have been extensively studied and modelled for repository-specific applications. Others, such as layered double hydroxides, have been studied primarily for application in groundwater remediation, particularly for the removal of the arsenate and phosphate oxyanions, which are not considered critical in SFL. Various materials do not meet the SKB concept requirements. For example, activated carbon is comprised of organic material, which can complex with and prevent the adsorption of nuclides that would otherwise be adsorbed to the bentonite, backfill, or bedrock. Then, some materials, such as surfactant-modified zeolites, are industrially manufactured, and thus their long-term stability can be assessed only through laboratory studies – without the additional support from observations of natural analogues. It should be noted that this is not a comprehensive list of all available ion adsorbents but rather those within the scope of this review. There is a general interest in zeolites and bentonite as adsorbents, and thus these are included in the report.

**Table 5-1. List of adsorbing materials categorized by relevance to this review and section of discussion.**

Type of Adsorbent	Material	Section
Cation Exchangers	Bentonite	5.2
	Zeolites	5.3
Anion Adsorbents	Layered double hydroxides	5.4
Amphoteric Adsorbents	Metal oxides and hydroxides	5.5
Mineralogically Complex	Red mud	5.6
	Zero-valent iron/Iron minerals	5.7
Used in environmental remediation, but not further described in present report	Activated carbon	–
	Biomaterials	–
	Waste materials	–
	Resins	–
	Fly ash	–
	Surfactant-modified zeolites	–

## 5.2 Bentonite

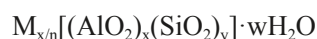
Bentonite clay is already integral to the sealing and sorption of radionuclides in the KBS-3 concept. The primary constituent of bentonite is the mineral montmorillonite (65 to 90 wt%). The SKB reference MX-80 bentonite contains 80 wt% montmorillonite, which has the formula  $(\text{Si}_{3.97}\text{Al}_{0.03})(\text{Al}_{1.55}\text{Fe}^{3+}_{0.19}\text{Ti}_{0.005}\text{Mg}_{0.25})\text{O}_{10}(\text{OH})_2\text{Na}_{0.23}\text{K}_{0.005}\text{Mg}_{0.01}\text{Ca}_{0.025}$  (Karlund 2010). A sketch of this structure is shown in Figure 5-1. It is a unit made of an alumina octahedral sheet sandwiched between two silica tetrahedral sheets. A permanent negative lattice charge arises when trivalent Al is isomorphously substituted for tetravalent Si in the tetrahedra and divalent cations (e.g. Mg, Fe) for trivalent Al in the octahedra. Excess cations in solution are then held electrostatically around the outside of the Si-Al-Si clay units to maintain charge neutrality. The electrostatically bound cations can exchange with cations in solution. This cation exchange mechanism is responsible for approximately 90% of the cation exchange capacity (CEC) of the montmorillonite (Bradbury and Baeyens 2011).

The CEC of montmorillonites are high,  $\sim 1$  Eq/kg, implying that the CEC of bentonite is significant, also. This quality, alongside its high swelling capacity and very low transmissivity to water movement, make it a very effective diffusion barrier. However, the structure and negative lattice charge as described above are ineffective as adsorptive barriers to the diffusive activity of redox insensitive anions, such as  $\text{Cl}^-$ . Bradbury and Baeyens (2011) reported  $\text{Cl}^-$  to have exhibited anion exclusion during sorption experiments. That is, the negatively-charged surface repelled  $\text{Cl}^-$  anions, forcing them out of the pore walls to where the water velocity is faster.

## 5.3 Zeolite

The study of zeolites is an interdisciplinary field of science which has over the years amassed an impressive number of publications. For this section on zeolites, the main sources of information are Dyer (2000), Gottardi (1978), Vaughan (1978) and Breck (1974). For information regarding the role of natural zeolites in repositories and other industrial applications, the reader is referred to reviews by Savage (2011) and Mumpton (1999), and references therein.

A zeolite is a three-dimensional network of  $\text{AlO}_4$  and  $\text{SiO}_4$  tetrahedra linked to each other by sharing all of the oxygen molecules. The general structure formula for the unit cell is:



Where M is a cation of valence n, where  $\text{M}^+ = \text{Na}^+$  or  $\text{K}^+$  and  $\text{M}^{2+} = \text{Mg}^{2+}$ ,  $\text{Ca}^{2+}$ , or  $\text{Fe}^{2+}$ . M cations are exchangeable, but their location within the structure determines their potential of exchange. The ratio of y/x (silica to alumina tetrahedral) determines the overall charge. Natural zeolites reach a ratio of 5, but values of 1000 can be obtained in some synthetic structures. W is the number of water molecules, which gives an idea of the volume of the channels in relation to the total volume. It does normally not exceed half the number of framework oxygen atoms.

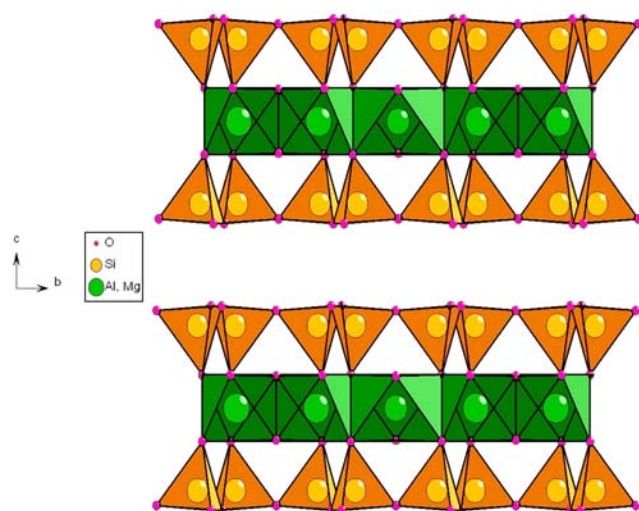


**Figure 5-1.** Sketch of the structure of montmorillonite (Bradbury and Baeyens 2011).

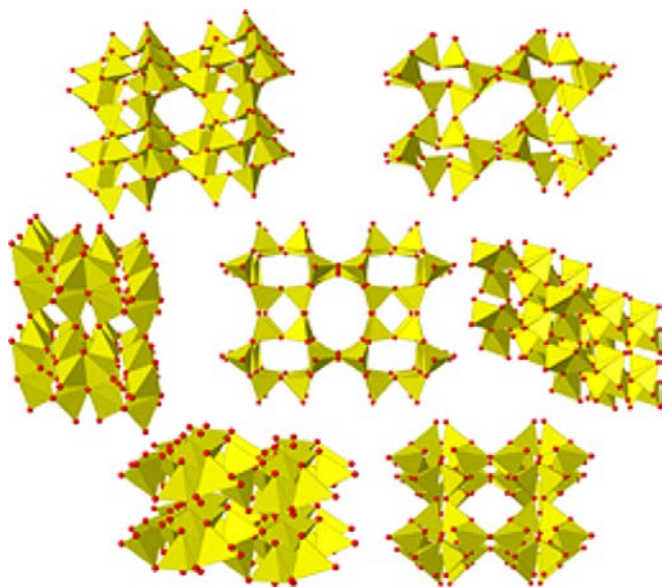


**Figure 5-2.** Example of variety in zeolite structures, yellow silicate tetrahedra connected by red oxygen atoms (Treacy 2010).

Over 30 species of zeolites occur in nature, and many that have no natural counterpart have been synthesized. Nearly 100 different frameworks have been crystallographically defined for zeolites and related structures. Some examples of zeolite structures are provided in Figure 5-2.

The retention potential of a zeolite depends on the structural and physico-chemical properties. A zeolite may retain nuclides through cation exchange, surface complexation, and incorporation into the zeolite structure during formation. Sorption-relevant zeolite properties include:

#### *Si/Al ratio*

Since it determines the fixed charge, which in turn largely determines the total cation exchange capacity: the lower the ratio, the higher the exchange capacity.

#### *Aperture size of the pores and internal channel structure*

Limits the maximum diameter of cations that can get into the channel systems of the zeolite; the size of the aperture is governed by the number of oxygen atoms in the rings that form the zeolite channel.

#### *Void volume or free space/framework density*

The smaller the cation, the greater the void volume and the water capacity. Related to the framework density, which in turn is related to the pore volume. Measure of the number of cations that can be hosted by the zeolite: the ion exchange of smaller (out-going) cations against larger (in-going) cations can be incomplete because the zeolite channel or cavity cannot accommodate all of the larger cations.

#### *Particle size*

Determines the specific surface area: the lower the particle size, the higher the specific surface area.

#### *Variable charge (hydroxyl groups at external and internal surfaces)*

Charge on zeolites may also arise due to pH dependent silanol ( $-\text{SiOH}$ ) and aluminol ( $-\text{AlOH}$ ) hydroxyl groups, which are available for surface adsorption and complexation. Lanthanides and actinides are believed to be retained only by surface complexation reactions since they occur under forms which are too large to penetrate the zeolite frameworks. Assuming that zeolites have a hydroxyl functional group density that is comparable to amorphous  $\text{SiO}_2$ , the complexing capacity



of the hydroxyl groups is one order of magnitude lower than the permanent negative charge originating from isomorphic substitution. It is expected that retention of radionuclides by surface complexation reactions will be small.

Zeolites can exhibit very high selectivities and high capacities (examples provided in Table 5-2), their cation capacities being a function of the extent of aluminium substitution into the framework. However, as is the case with clays, full exchange cannot be attained in some zeolites. For example, some zeolites are affected by ‘ion-sieving’, which occurs partially due the presence of ingoing ions that are too large to pass through the channel dimensions. Their application has also been restricted by their instability in acid environments.

In a repository making extensive use of cementitious materials, a high pH pore fluid can be expected upon dissolution. Through dissolution-precipitation reactions in the alkaline plume, zeolite minerals are expected to form (see review by Savage, 2011).

The zeolites found most relevant for the present review are listed in Table 5-2 based on the following criteria:

- They are found in nature.
- They are commonly formed at temperatures below 80°C.
- They represent different structural groups of zeolites.

Each zeolite is observed to have a unique, general selectivity series, reported in Table 5-2.

**Table 5-2. Cation exchange capacity and selectivity series of some zeolites.**

Zeolite	Cation Exchange Capacity*	Selectivity Series**
Phillipsite	4.67 meq/g	$\text{Cs}^+ > \text{Na}^+ > \text{Sr}^{2+} = \text{Ca}^{2+}$ $\text{Cs}^+ > \text{K}^+ > \text{Rb}^+ > \text{Na}^+ > \text{Li}^+$ $\text{Ba}^{2+} > \text{Cs}^+ = \text{Rb}^+ = \text{K}^+ > \text{Na}^+ \gg \text{Li}^+$ Particular selectivity for $\text{Ba}^{2+}$ , $\text{Cs}^+$ , $\text{Rb}^+$ , and $\text{K}^+$ , but low $K_d$ values for $\text{Sr}^{2+}$ expected where $\text{K}^+$ and $\text{Na}^+$ are high
Analcime	4.95 meq/g	Channel diameter only 2.8 Å, so structure not accessible to cations with a large diameter $\text{Na}^+$ can be completely replaced with $\text{K}^+$ , $\text{Ag}^+$ , $\text{Ti}^+$ , $\text{NH}_4^+$ , and $\text{Rb}^+$ at elevated temperature Only negligible exchange with $\text{Li}^+$ , $\text{Cs}^+$ , $\text{Mg}^{2+}$ , $\text{Ca}^{2+}$ , and $\text{Ba}^{2+}$ Small amounts of $\text{Sr}^{2+}$ , $\text{Mg}^{2+}$ , $\text{Ni}^{2+}$ and $\text{Co}^{2+}$ exchanged Not expected to play important role in retention of released nuclides
Chabazite	4.95 meq/g	$\text{Ti}^+ > \text{Cs}^+ > \text{K}^+ > \text{Ag}^+ > \text{Rb}^+ > \text{NH}_4^+ > \text{Pb}^{2+} > \text{Na}^+ = \text{Ba}^{2+} > \text{Sr}^{2+} > \text{Ca}^{2+} > \text{Li}^+$ Large (hydrated) ions, such as $\text{La}^{3+}$ , are excluded by ion-sieve effect, indicating that trivalent actinides will not be able to exchange in the framework
Mordendite	2.62 meq/g	$\text{Cs}^+ > \text{K}^+ > \text{NH}_4^+ > \text{Na}^+ > \text{Ba}^{2+} > \text{Li}^+$ $\text{NH}_4^+ > \text{Na}^+ > \text{Mn}^{2+} > \text{Cu}^{2+} > \text{Co}^{2+} = \text{Zn}^{2+} > \text{Ni}^{2+}$
Clinoptilolite	2.63 meq/g	$\text{Cs}^+ > \text{K}^+ > \text{Sr}^{2+} = \text{Ba}^{2+} > \text{Na}^+ \gg \text{Li}^+$ $\text{Cs}^+ > \text{Rb}^+ > \text{K}^+ > \text{Na}^+ > \text{Sn}^{2+} > \text{Li}^+$ and $\text{Pb}^{2+} > \text{Ag}^+ > \text{Cd}^{2+} = \text{Zn}^{2+} = \text{Cu}^{2+} > \text{Na}^+$
Natrolite		No selectivity data found
Dachiardite		No selectivity data found

\*(Dyer 2000).

\*\* (Vaughan, 1978; Breck, 1974).

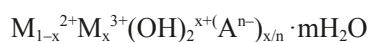
Zeolites are studied because of their ion exchange properties, and since their surfaces are negatively charged, the exchange of cations predominates. While capable of surface complexation reactions – and therefore pH-dependent anion adsorption – zeolites have a fairly low density of hydroxyl functional groups. Thus, retention by this mechanism will be small. As such, they appear to be inadequate sorbents for the nuclides and anionic complexes on which this SKB report focuses. Moreover, if  $K^+$  and  $Na^+$  ions are present at high concentrations, these will compete with the alkali (K, Rb, Cs) and alkaline earth metals (Sr, Ra) and reduce their distribution coefficients ( $K_d$ ). As for the heavy metals – transition elements (Nb, Mo, Mn, Tc, Pd, Ni, Zn, Ag, Sn, Pb) and the alkaline earth metals, cation sieving effects seriously hamper ion exchange and reduce the  $K_d$  values. One can attempt to predict whether a cation can penetrate into a zeolite structure on the basis of maximum ring size and ionic radius; however, such a prediction is complicated by the fact that cations often occur in hydrated form and zeolites can be deformed.

Still, zeolites can show reasonably to extremely high ion exchange capacities, hypothetically resulting in a high retention of released radionuclides. Additionally, their prevalence in nature may offer analogues for insight into their effectiveness and stability over the long-term. Some natural zeolites, such as clinoptilolite, chabazite, phillipsite, and mordenite have been employed in nuclear waste treatment to remove  $Cs^+$ ,  $Sr^{2+}$ , and other radionuclides from waste streams.

In case further investigations are warranted for retardation of cations by zeolites, a more detailed survey of specific zeolite types may be undertaken. Upon recognizing that a literature survey on the sorption properties of all known natural zeolites would be an enormous and time-consuming task, SKB may benefit from an approach, in which are considers whether specific cations can penetrate into a zeolite structure on the basis of ionic radius and maximum ring size. Consideration must be given to the facts that cations normally occur in hydrated form, one zeolite may have different channels of different aperture sizes, some actinide complexes are too large to penetrate the zeolite channels, etc. Additionally, the zeolite framework is not necessarily totally rigid and may be subject to small deformations.

## 5.4 Layered Double Hydroxide (LDHs)

Also called hydrotalcite-like compounds, those in this class of isostructural, two-dimensional nano-structured anionic clays vary in physicochemical properties. They are of interest because they exhibit the ability to capture organic and inorganic anions through the process of adsorption and ion exchange. Although they are relatively rare in nature, being associated with metamorphic rock formations or saline deposits (Mokaya 2000), they can be simple and economical to synthesize. The parent material is the naturally occurring mineral hydrotalcite, which has the formula  $Mg_6Al_2(OH)_{16}CO_3 \cdot 4H_2O$ . The structure has brucite-like sheets ( $Mg(OH)_2$ ) that are stacked atop each other and held together by hydrogen bonding. A positive charge arises when ions that have similar ionic radii to  $Mg^{2+}$  ( $M^{2+} = Mg^{2+}, Fe^{2+}, Co^{2+}$ , etc and  $M^{3+} = Al^{3+}, Cr^{3+}, Fe^{3+}$ , etc.) are accommodated in the holes of the close-packed configuration of OH groups in the brucite-like sheets. The positive charge is compensated by anions in the interlayer region between the brucite-like sheets. Figure 5-3 shows this structure, with the general formula:



Where:  $x = M^{3+}/(M^{2+}+M^{3+})$  and A = interlayer anion of valence n; ions that have similar ionic radii to  $Mg^{2+}$  can be accommodated in layers:  $M^{2+} = Mg^{2+}, Fe^{2+}, Co^{2+}$ , etc., and  $M^{3+} = Al^{3+}, Cr^{3+}, Fe^{3+}$ , etc.

Charge density and anion exchange capacity is controlled by varying the  $M^{2+}/M^{3+}$  ratio. The most common anion found in naturally occurring LDH is carbonate but halides, oxyanions, silicates, poly-oxometalate anions, complex anions, and organic anions can also be incorporated. For example, another class of LDHs, which contains monovalent and trivalent matrix cations, such as  $LiAl_2(OH)_6^+A^- \cdot mH_2O$  has been prepared and appears to intercalate monovalent anions. Upon the anoxic corrosion of zero-valent iron to the +2 and +3 oxidation states, an LDH called green rust (or the mineral fougérite where natural processes are occurring) can precipitate. Further details can be found in Section 5.6.



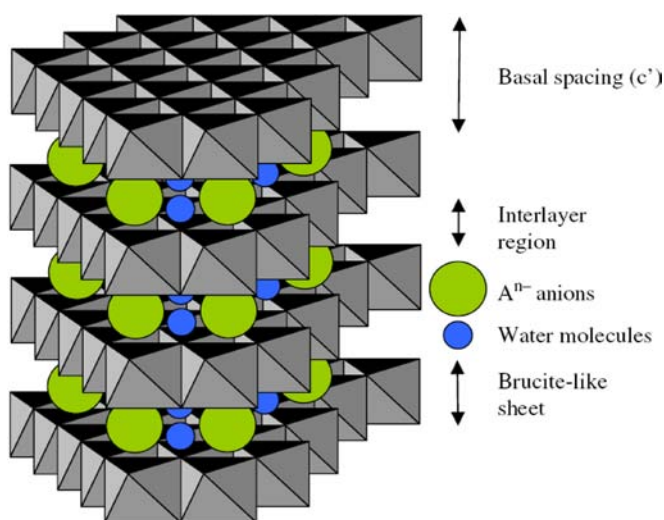


**Figure 5-3.** Schematic representation of the LDH structure (Goh et al. 2008).

The ion exchange reaches a maximum when the interlayer region is large enough for the oxyanions to fit into the region for exchange process. Molybdate has an ionic radius of 0.246 nm, carbonate 0.189 nm, iodate 0.218 nm, pertechnetate 0.252 nm, selenate 0.243, and chromate 0.240 (Goh et al. 2008 and references therein). Additionally, Goh et al. (2008) provide a list of oxyanions which have been investigated for their adsorption characteristics with various LDHs and the corresponding reference. Notably, Zhang and Reardon (2003) investigated the adsorption characteristics of molybdate onto uncalcined hydroxide-Ca-Al LDHs and carbonate-Ca-Al LDHs. Toraishi et al. (2002) investigated those of iodate onto uncalcined carbonate-Mg-Al LDHs (commercial) and nitrate-Mg-Al LDHs. Kang et al. (1996 and 1999) and Wang and Gao (2006) studied the adsorption characteristics of pertechnetate onto uncalcined and calcined Mg-Al LDHs and uncalcined M(II)-M(III) (where M(II) = Co, Ni, Cu, Fe, Cd, Pd, and Mn and M(III) = Al, Fe, Cr, V, Y, Yb, La, Ga, and Bi) LDHs, respectively. Other anions investigated include vanadate, perhenate, nitrate, borate, selenate, selenite, phosphate, chromate, arsenate, and arsenite.

Wang and Gao (2006) synthesized a large set of LDH materials with various combinations of metal cations, interlayer anions, and molar ratios of divalent cations M(II) to trivalent cations M(III) and then tested them for their sorption capabilities for pertechnetate ( $\text{TcO}_4^-$ ). The Ni-Al LDH with a Ni/Al ratio of 3:1 exhibited the highest sorption capability for  $\text{TcO}_4^-$ , with a  $K_d$  value of 307 mL/g at a pH of 8. The sorption of  $\text{TcO}_4^-$  on M(II)-M(III)- $\text{CO}_3$  LDHs may have been dominated by the edge sites of LDH layers and correlated with the basal spacing of the materials, which increases with the decreasing radii of both divalent and trivalent cations. Sorption reached a maximum when the layer spacing was just large enough for a pertechnetate to fit into a cage space among three adjacent octahedral of metal cations and an interlayer anion. Sorption increases with the crystallinity of the materials, the best crystalline LDH generally being obtained with a M(II)/M(III) ratio of 3:1 (Wang and Gao 2006). Pertechnetate has a similar radius as molybdate, although molybdate is smaller and more negatively charged, which suggests that molybdate may adsorb to the Ni-Al LDH more efficiently than pertechnetate.

Zhang and Reardon (2003) compared the removal of borate ( $\text{B(OH)}_4^-$ ), selenate ( $\text{SeO}_4^{2-}$ ), chromate ( $\text{CrO}_4^{2-}$ ), and molybdate ( $\text{MoO}_4^{2-}$ ) by hydrocalumite ( $\text{Ca}_4\text{Al}_2\text{CO}_3(\text{OH})_{12} \cdot 5\text{H}_2\text{O}$ ), which is composed of portlandite-like principal layers with one-third of the  $\text{Ca}^{2+}$  sites being occupied by  $\text{Al}^{3+}$ . Although not LDHs, hydrocalumite is an anionic clay and an analogue for hydrotalcite. Furthermore, a principal objective of the study was to examine the anion uptake behaviour in terms of the structural characteristics, anion coordination, size, and electronegativity. Hydrocalumite selected for the oxyanions in the order  $\text{SeO}_4^{2-} > \text{CrO}_4^{2-} > \text{MoO}_4^{2-} > \text{B(OH)}_4^-$ . Selenate and chromate occur in regular tetrahedrons. Molybdate has the largest bond length of these anions, and its tetrahedron can be coordinated irregularly.

Thus, in addition to the charge and ionic radius of the ions and the basal spacing of the anionic clay, sorption will depend on the compatibility of geometries. For example, carbonate is preferred in hydrotalcite because the trigonal planar carbonate anions are oriented parallel to the principle layers, whereas tetrahedral sulphate anions are randomly oriented (Zhang and Reardon 2003). Zhang and Reardon (2003) also present anion sorption data and analysis for the mineral ettringite, mentioned in Section 6.

More work should be focused on determining their  $\text{pH}_{\text{pzc}}$ , yet Goh et al. (2008) reported the following values, presented in Table 5-1.

**Table 5-3. Reported  $\text{pH}_{\text{pzc}}$  values of LDHs found in LDH literature review (Goh et al. 2008).**

Types of LDHs	$\text{pH}_{\text{pzc}}$
Uncalcined Mg-Al LDHs	12.0–12.5
Uncalcined Mg-Fe LDHs	8.9
Uncalcined chloride-Mg-Al-Fe LDHs	10.9–11.1
Uncalcined Mg-Fe LDHs	8.7
Uncalcined chloride-Li-Al LDHs	7.2
Uncalcined chloride-Zn-Al LDHs	10.4–11.0
Uncalcined chloride-Zn-Al-Fe LDHs	9.3–10.0

## 5.5 Hydrous metal oxide (amphoteric)

Oxide surfaces, unless highly dried, are usually covered with hydroxyl groups. These groups are formed by dissociative chemisorptions of water due to the undercoordinated metal ions (e.g.  $\text{Si}^{4+}$ ,  $\text{Al}^{3+}$ ,  $\text{Fe}^{3+}$ ) occurring on the top layer of the oxide surfaces. The exposed ions react with water molecules to form surface OH groups in an attempt to complete the coordination sphere (Tombácz 2002). The retained OH groups enable the oxide to function as either anion exchangers, via replaceable  $\text{OH}^-$  groups, or as cation exchangers when the OH groups ionize and release  $\text{H}^+$  ( $\text{H}_3\text{O}^+$ ) ions. The tendency to ionize depends on the basicity of the metal atom attached to the OH group, and the strength of the metal-oxide bond relative to the O-H bond. Some materials are amphoteric, that is, they are able to function as both anion and cation exchangers, depending upon solution pH. Capacities lie in the range 0.3–0.4 meq/g. Hydroxyl groups can coordinate with the metal ions at the oxide surface either during hydration, when the surface is exposed to moisture and water is chemisorbed, converting the top layer of oxide ions to hydroxyl ions, or when the oxide precipitates from water, retaining OH groups on the surface. The freshly precipitated oxides are poorly crystalline, and usually occur as very small particles with loosely bound water molecules held in their structures, becoming more crystalline as they age (Dyer 2000).

Well-known trivalent hydrous oxides are those of iron and aluminium, each producing more than one hydrous oxide. Examples are  $\alpha$ -FeOOH (goethite),  $\beta$ -FeOOH, and  $\gamma$ -FeOOH (lepidocrocite). Adsorption of simple inorganic anions and oxyanions on iron oxides has been widely investigated, and Table 5-4 provides a list and references focused around those of interest to this study. Of the aluminium compounds,  $\alpha$ - $\text{Al}_2\text{O}_3$  (corundum),  $\alpha$ -AlOOH (diaspore), and  $\alpha$ - $\text{Al}(\text{OH})_3$  (gibbsite) exhibit exchange. The aluminium compounds have been studied thoroughly because of their use as catalysis support materials and chromatographic substrates. Figure 5-4 shows the capacity of a commercial alumina as a function of pH and the transition from anion exchange to cation exchange at  $\sim\text{pH } 7$ . In that study, reported by Dyer (2000), the compound is not specified, but it is likely a catalytic alumina, usually  $\gamma$ - $\text{Al}_2\text{O}_3$ , with a very high surface area. Gallium, indium, chromium, bismuth, antimony, and lanthanum are other elements whose trivalent oxides display ion exchange properties (Dyer 2000).

**Table 5-4. Adsorption studies of relevant inorganic anions on iron oxides (Cornell and Schwertmann 2003).**

Oxide	Anion	Nr of studies reported by Cornell and Schwertmann (2003)
<b>Goethite</b>	Carbonate	4
	Chloride	1
	Iodate	1
	Molybdate	4
<b>Ferrihydrite</b>	Carbonate	1
<b>Hematite</b>	Molybdate	2
<b>Magnetite</b>	Chloride	1
	Molybdate	1

Hydrous oxides of tetravalent manganese, silica, tin, titanium, thorium, and zirconium also exhibit amphoteric ion exchange properties. Zirconia and titania have been of interest for nuclear waste treatment, alongside manganese dioxide, for its high capacity for strontium isotopes (Dyer 2000). Figure 5-5 shows the capacity of zirconium and thorium oxides for  $\text{Cl}^-$ ,  $\text{Na}^+$ , and  $\text{Cs}^+$  as a function of pHs and the pHs at which each material transitions from anion to cation exchange, ~8–10.

Figures 5-4 and 5-5 show some of the variation between the exchange properties of different metal oxides as ion adsorbents. If the objective is to adsorb anions, then a material with a higher  $\text{pH}_{\text{pzc}}$ , such as the tetravalent metal oxides shown in Figure 5-5, may be more effective adsorbents. While their capacity is generally lower than that of the alumina shown in Figure 5-4, they have a greater capacity for anions in more alkaline conditions. However, the alumina adsorbent shown in Figure 5-4 has higher uptakes of anions at a low pH and of cations at a high pH, which may be an attractive property if the objective is to adsorb cations or to anticipate a variation in pH conditions.

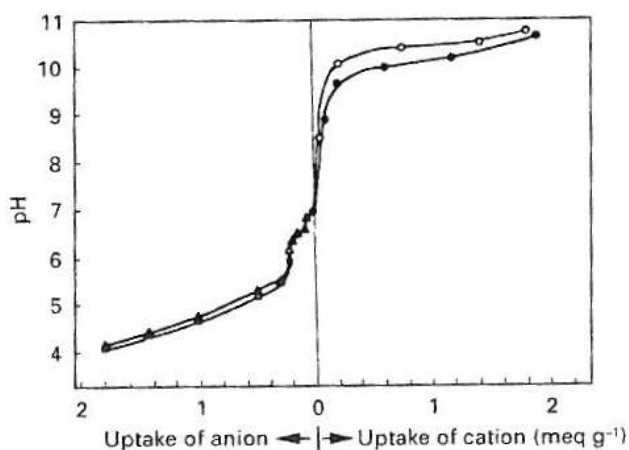


**Figure 5-4.** Exchange capacity of a commercial alumina, showing uptake of  $\text{Cl}^-$  and  $\text{NO}_3^-$  at  $\text{pH} < 7$ –8 and uptake of  $\text{Li}^+$  and  $\text{K}^+$  above this pH (Dyer 2000).

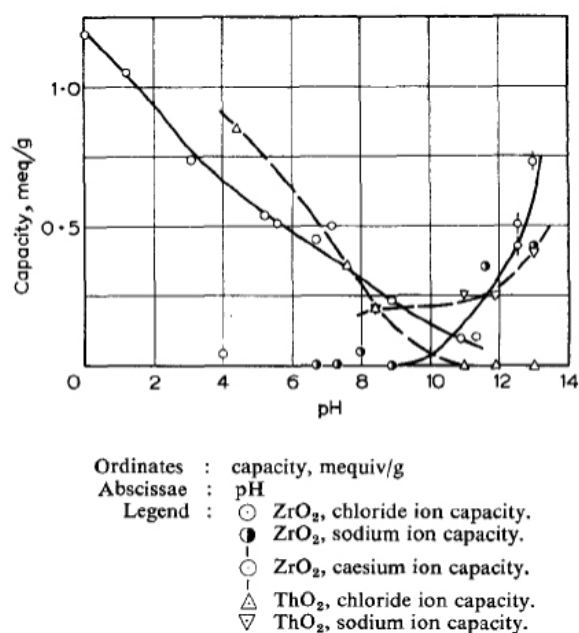


**Figure 5-5.** Anion and cation exchange capacity of ZrO<sub>2</sub> and ThO<sub>2</sub> as a function of pH, the  $pH_{pzc}$  appearing around pH ~9–10 (Amphlett et al. 1958).

Hydrous tin dioxide, or SnO<sub>2</sub>·H<sub>2</sub>O is also interesting because it is more amphoteric than the hydrous oxides of titanium, manganese, and zirconium. These showed virtually no sorption for anionic iodine species at higher pH values (White and Rautiu 1997 and references therein). Hydrous tin dioxide has been shown to be a very good cation exchanger, but the anionic sorption properties were less extensively studied as of 1997 (White and Rautiu 1997 and references therein). It has an ion exchange capacity of 1.49 meq/g and its  $pH_{pzc} = 4.0$ . Figure 5-6 shows the uptake of the anions included in this study, as a function of pH. Based on their valence and hydrolysis constant ( $K_a$ ) properties, Cl<sup>-</sup> would be intuitively expected to lie between F<sup>-</sup> and I<sup>-</sup>.

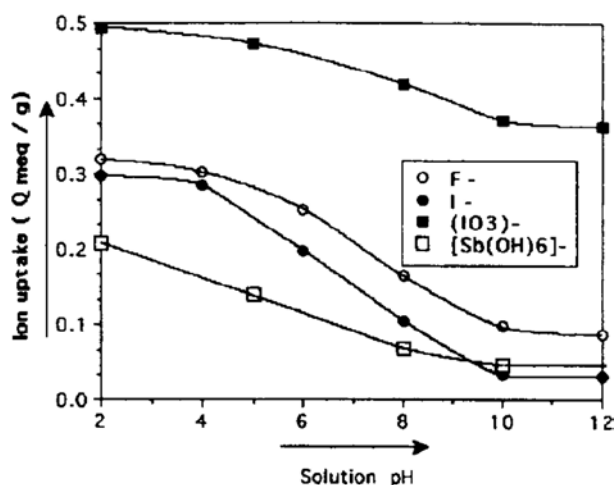


**Figure 5-6.** Uptake of F<sup>-</sup>, I<sup>-</sup>, IO<sub>3</sub><sup>-</sup>, and Sb(OH)<sub>6</sub><sup>-</sup> by hydrous tin dioxide as a function of pH (White and Rautiu 1997).

## 5.6 Red Mud

Red mud is a waste product derived from the digestion of bauxite, an aluminium ore. The caustic NaOH required in this process results in a strongly alkaline (pH 10–12.5) waste product. Since this poses an environmental hazard, the red mud waste is disposed of in waste dumps that cover large areas of land, the costs of which contribute significantly to the production cost of alumina. The red mud is composed primarily of fine particles of silica, aluminium, iron, calcium, and titanium oxides and hydroxides. Its potential as a cost-effective sorbent has been investigated for application to the immobilization of heavy metals in contaminated soils and their removal from waste water and acid mine drainage (Santona et al. 2006). Its sorption properties have also been studied for application as a barrier in a shallow-land burial site for low-level wastes (Apak et al. 1995).

The exact composition of the red mud produced depends on the particular chemical and mineralogical composition of the bauxite before digestion. Some examples given by Palmer et al. (2009) are shown in Table 5-5.

Bauxite refinery residues are initially a slurry, the liquid portion of which is suitable for discharge after treatment. The solid residue must be neutralized, and this can be done using either an acid treatment (Santona et al. 2006) or neutralization by seawater. Beyond the range in mineralogy shown above and the implication of such on adsorption mechanisms and efficiency, each treatment can induce an array of physical and chemical changes in the red mud. Consequently, such further affects the sorption parameters, as discussed below.

### 5.6.1 Untreated red mud

Castaldi et al. (2010a, b) published two separate articles testing the sorption of the anions  $\text{PO}_4^{3-}$  and  $\text{AsO}_4^{3-}$  onto red mud at pH 10, 7, and 4. Table 5-3 shows the corresponding mineralogical compositions at these pHs. Results suggested that the anions preferentially adsorbed on the Fe-Al oxides and hydroxides (hematite, boehmite, and gibbsite). As usual, the sorption decreased as the pH increased. Also, the phosphate adsorbed to the red mud was three times higher than arsenate at pH 4.0, and consistently higher at 10 and 7. This may be due to the anions having different sorption, precipitation, and diffusion mechanisms in interacting with the red muds.

- Phosphate sorbed on red mud at pH 4.0 was three times higher with respect to arsenate; pH 7.0 P-RM = 1.078 mmol/g and As(V)-RM = 0.17 mmol/g; pH 10.0 P-RM = 0.240 mmol/g and As(V)-RM = 0.12 mmol/g (Castaldi et al. 2010a, b).

**Table 5-5. Mineralogy of bauxite from various locations (Palmer et al. 2009).**

Minerals	Weipa	Darling Range	Guinea Boké	Jamaica	India	Hungary Iszkaszentgyogy	Greece
Gibbsite, $\text{Al}(\text{OH})_3$	58.3	51.1	71.9	64.7	59.2	24.5	0
Boehmite, $\text{AlO}(\text{OH})$	12.5	0.4	14.4	3.6	7.8	30	3.0
Diaspore, $\text{AlO}(\text{OH})$	0.2	0.5	0.3	0.2	1.2	1.5	60.0
Kaolin, $\text{Al}_2\text{O}_3 \cdot 2\text{SiO}_2 \cdot 2\text{H}_2\text{O}$	10.3	6.5	2.3	3.4	5.6	12.7	0
Quartz, $\text{SiO}_2$	Trace	17.4	0	0.5	1.4	0.5	3.0
$\text{Fe}_2\text{O}_3$	10.6	7.2	2.6	15.8	10.7	5.2	21.0
Goethite, $\text{FeO}(\text{OH})$	3.9	9.5	2.4	5.3	6.2	13.8	4.0
Anastase, $\text{TiO}_2$	2.0	1.0	2.7	2.2	6.0	1.8	3.0
Rutile, $\text{TiO}_2$	0.7	0	0.8	0.2	0.5	0.6	0
$\text{P}_2\text{O}_5$	0.1	NR	0	0.7	NR	NR	NR
CaO	0.1	0	0.1	0.9	NR	0.6	0.7
	<b>98.7</b>	<b>93.7</b>	<b>97.5</b>	<b>97.8</b>	<b>98.6</b>	<b>91.2</b>	<b>94.7</b>

NR = Not reported.

**Table 5-6. Chemical parameters and mineralogy of an untreated red mud that was investigated for cation and anion adsorption potential (Santona et al. 2006 and Casaldi et al. 2010).**

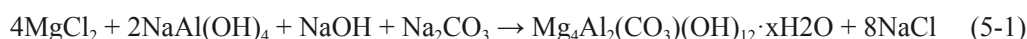
Red Mud (Not treated)	Santona et al. (2006)			Castaldi et al. (2010b)							
Chemical parameters						pH adjustment					
pH	11.5			11.1		10	7		4		
SBET (m²/g)	18.87			19.5		21.4	23.6		25.5		
pHpzc				4.77		–	–		–		
CEC (mmol/kg)	106.5										
Crystalline Phases (wt%)											
Cancrinite [Na <sub>6</sub> Ca <sub>1.5</sub> Al <sub>6</sub> Si <sub>6</sub> O <sub>24</sub> (CO <sub>3</sub> ) <sub>1.6</sub> ]	51.0			4.0		4.0	3.5		n.d.		
Sodalite [Na <sub>8</sub> (Cl,OH) <sub>2</sub> Al <sub>6</sub> Si <sub>6</sub> O <sub>24</sub> ]	–			20.0		24.0	24.0		22.0		
Hematite [Fe <sub>2</sub> O <sub>3</sub> ]	27.0			44.0		42.0	42.0		49.0		
Gibbsite [Al(OH) <sub>3</sub> ]	3.0			4.0		4.0	4.0		4.0		
Boehmite [AlO(OH)]	9.0			12.0		12.0	12.0		8.0		
Anatase [TiO <sub>2</sub> ]	3.0			4.5		4.0	4.0		4.0		
Quartz [SiO <sub>2</sub> ]	2.0			6.0		5.0	5.5		6.0		
Ca-Fe-V-oxide	3.5			–		–	–		–		
MgO	1.5			–		–	–		–		
Andradite [Ca-Fe-Al-Si oxide]	–			5.5		5.0	5.0		5.5		
	100.00			100.00		100.00	100.00		98.50		
Ions investigated	Pb	Cd	Zn	PO <sub>4</sub> <sup>3-</sup>	AsO <sub>4</sub> <sup>3-</sup>	PO <sub>4</sub> <sup>3-</sup>	HAsO <sub>4</sub> <sup>2-</sup> +H <sub>2</sub> AsO <sub>4</sub> <sup>-</sup>	PO <sub>4</sub> <sup>3-</sup>	HAsO <sub>4</sub> <sup>2-</sup> +H <sub>2</sub> AsO <sub>4</sub> <sup>-</sup>	PO <sub>4</sub> <sup>3-</sup>	H <sub>2</sub> AsO <sub>4</sub> <sup>-</sup>
Langmuir (x/m = KbC/(1+KC))	pH=5.5 – 5.9										
Parameters: b (mmol/g)	1.88	1.35	2.47	–	–	0.24	0.12	1.078	0.17	R2 values do not fit L or F isotherm	
K (L/mmol)	0.75	0.79	1.53	–	–	1.181	4.55	0.032	2.45		
R²	0.94	0.96	0.96	–	–	0.98	0.94	0.97	0.85		
% Extracted using:											
H <sub>2</sub> O	<.01	<.01	<5	H <sub>2</sub> O		<15%	0%	<15%	<15%	<5%	<15%
Ca(NO <sub>3</sub> ) <sub>2</sub>	0	<1.5	<1.5	(NH <sub>4</sub> ) <sub>2</sub> SO <sub>4</sub>		0%	<10%	<5%	<10%	<1%	<10%
EDTA(max)	80	75	57	NaH <sub>2</sub> AsO <sub>4</sub>		<20%	–	15%	–	<1%	–
				NH <sub>4</sub> H <sub>2</sub> PO <sub>4</sub>		–	25%	–	20%	–	<20%
				NH <sup>4+</sup> -oxalate		<15%	<40%	<10%	<30%	1%	<35%
				NH4+-oxalate buffer + ascorbic acid		10%	20%	0%	20%	0%	25%

### 5.6.2 Acid-treated red mud

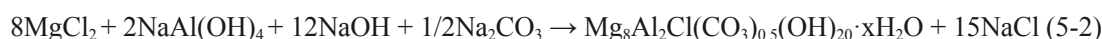
Cancrinite is the primary mineral before and after acid treatment. It has an open porous structure and can be considered as a material with zeolite-like properties. After treatment by acid, some cancrinite dissolves and its hematite content increases. Santana et al. (2006) tested the sorption of the cations Zn, Pb, and Cd and found that they primarily adsorbed to the cancrinite and hematite. At the pH of the experiment (5.5–5.9), the negatively charged surface of the cancrinite was neutralized by the incorporation of metal adsorbed with outer-sphere bonds into the cages and channels of the cancrinite framework. Despite the acid-treated red mud having more hematite than the not acid-treated, the cancrinite in the untreated red mud enabled it to adsorb more cations. Acid treatment with HCl decreased the red mud's capacity to adsorb the cations by 30%. More Zn was adsorbed than Pb or Cd, possibly due to its higher charge density (Santana et al. 2006). Table 5-7 shows the properties, mineralogy, and sorption experiment results of an acid-treated red mud.

### 5.6.3 Seawater-treated red mud

A number of alumina refineries, one being Queensland Alumina Ltd., have implemented seawater neutralization of red mud having found the method superior to treatment by strong acids (Palmer et al. 2009). Such is currently the preferred industrial neutralization method. The alkalinity is neutralized in the reaction:



at pH > 13 (Mg:Al = 2:1) and:



at pH 8 (Mg:Al = 4:1).

These result in the formation of Mg, Ca, and Al hydroxide and carbonate minerals, such as hydrotalcite, an LDH. Seawater neutralized red mud consists of both the Mg:Al = 2:1 and the Mg:Al = 4:1 varieties. (Notice the Cl and CO<sub>3</sub> intercalated into the hydrotalcite structure in the second

**Table 5-7. Chemical parameters, mineralogy, and sorption experiment results of an acid-treated red mud (Santana et al. 2006).**

Red Mud (Acid-treated)	Santona et al. (2006)			
pH	7			
S <sub>BET</sub> (m <sup>2</sup> /g)	25.16			
pHpzc	8-8.5 (references therein)			
CEC (mmol/kg)	98.2			
<b>Crystalline Phases (wt%)</b>				
Cancrinite [Na <sub>6</sub> Ca <sub>1.5</sub> Al <sub>6</sub> Si <sub>6</sub> O <sub>24</sub> (CO <sub>3</sub> ) <sub>1.6</sub> ]	42.0			
Hematite [Fe <sub>2</sub> O <sub>3</sub> ]	31.0			
Gibbsite [Al(OH) <sub>3</sub> ]	3.0			
Boehmite [AlO(OH)]	9.6			
Anatase [TiO <sub>2</sub> ]	3.0			
Quartz [SiO <sub>2</sub> ]	3.0			
Ca-Fe-V-oxide	4.0			
MgO	3.0			
	98.6			
<b>Ions investigated:</b>	<b>Pb</b>	<b>Cd</b>	<b>Zn</b>	
<b>Langmuir (x/m = KbC/(1+KC))</b>				
Parameters:				
b (mmol/g)	0.77	0.91	1.59	
K (L/mmol)	1.42	2.07	2.1	
R <sup>2</sup>	0.87	0.77	0.97	
% Extracted using:				
H <sub>2</sub> O	<15	<10	<15	
Ca(NO <sub>3</sub> ) <sub>2</sub>	15	<10	<15	
EDTA(max)	65	10	28	



equation.) Hydrotalcites prefer to form with divalent anions over monovalent anions and shows the greatest affinity for anions of high charge density. The order of monovalent anions is  $\text{OH}^- > \text{F}^- > \text{Cl}^- > \text{Br}^- > \text{NO}_3^- > \text{I}^-$  while the order of divalent anions is  $\text{CO}_3^{2-} > \text{SO}_4^{2-}$ . Carbonate is the preferred anion for intercalation and is very difficult to exchange (Palmer et al. 2009).

Thermally activated seawater neutralized red mud removes at least twice the concentration of anionic species than thermally activated red mud due to the formation of 40–60% Bayer hydrotalcite. Palmer et al. (2010) synthesized hydrotalcites of Mg:Al ratios 2:1, 3:1, and 4:1 and tested the removal of varying concentrations (5, 25, 50, 75, and 100 ppm) of arsenate, vanadate, and molybdate. In individual aqueous systems, nearly 100% of the arsenate and vanadate were removed at each concentration, while removal of molybdate decreased from 100% at 5 ppm to ~85% at 100 ppm. In the same aqueous system, where each solution contained equivalent concentrations of each anionic species, arsenate and vanadate had a higher affinity for hydrotalcite. Arsenate and vanadate out-competed molybdate for the positive sites in the inter-layer and on the external surface, the reason being attributed to molybdate's larger anionic radius and smaller charge density. The 3:1 hydrotalcite removed molybdate most efficiently from the molybdate aqueous system, while the 4:1 hydrotalcite increased the percentage of all anions removed from solution in the same aqueous system (Palmer et al. 2010).

#### 5.6.4 Applied to nuclear waste disposal

Apak et al. (1995) studied the adsorption affinities and the parameters affecting the sorption of Cs-137 and Sr-90 onto red mud in order to assess its potential for use as a barrier in the shallow-land burial of low-level radioactive waste. The red mud in this study had the chemical composition shown in Table 5-5 before being washed thoroughly with water to a neutral pH ( $R_w$ ) then dried and sieved. A fraction of this was then treated with HCl ( $R_a$ ), another fraction of which was further subjected to heat-treatment at 600°C to obtain the  $R_{ah}$  sorbents. Like the derivations obtained from the treatment methods discussed in previous sections, the differences in the physical and chemical properties of the  $R_w$ ,  $R_a$ , and  $R_{ah}$  induced sorption experiment results that varied by treatment. Work on  $\text{Cs}^+$  and  $\text{Sr}^{2+}$  adsorption to the red muds included studies on the effects of temperature, inert electrolytes, and pH dependency on sorption and the determination of adsorption isotherms and desorption efficiency.

$\text{Cs}^+$  adsorption to  $R_w$  decreased from ~60% to ~45% as temperature increased from 25°C to 75°C.  $\text{Sr}^{2+}$  adsorption onto  $R_w$  and  $R_a$  was rather independent of temperature, but adsorption to  $R_{ah}$  increased from ~65% to 85% as the temperature increased from 25°C to 75°C. In the presence of an NaCl (inert electrolyte) solution,  $\text{Cs}^+$  adsorption decreased as the NaCl concentration increased. This could be due to the coverage of adsorption sites by  $\text{Na}^+$  ions. However, exchange of  $\text{Cs}^+$  with  $\text{Na}^+$  ions on the aluminosilicate (cancrinite and sodalite) units could also be occurring.  $\text{Na}^+$  did not compete with  $\text{Sr}^{2+}$  for adsorption to  $R_w$ , which indicated that  $\text{Sr}^{2+}$  was bound by forces stronger than electrostatic ion uptake. A greater extent of competition of  $\text{Na}^+$  with  $\text{Sr}^{2+}$  was observed for the  $R_a$  and  $R_{ah}$ , a possible indication of an increase in the ion exchange sorption mechanism relative to that of surface complexation. Figure 5.7 shows the dependency of  $\text{Cs}^+$  and  $\text{Sr}^{2+}$  sorption on pH. For each type of red mud,  $\text{Cs}^+$  adsorption shows a maximum at a neutral pH, while  $\text{Sr}^{2+}$  adsorption increased with pH.

Table 5.5 shows the Langmuir parameters for  $\text{Cs}^+$  and  $\text{Sr}^{2+}$  adsorption and the adsorption capacity at saturation of each type of red mud in neutral solution. It can be seen that the  $\text{Sr}^{2+}$  capacity is higher than  $\text{Cs}^+$  in each type of sorbent, and in exceeding those expected from pure ion exchange may indicate the occurrence of surface complexation by hydrous oxide-like sorbents.  $\text{Cs}^+$  also predominantly sorbs by surface complexation, though another mechanism, possibly ion exchange, may accompany it at high sorbent loadings. Acid- and heat-treated red muds are more effective in  $\text{Cs}^+$  removal than water-washed red muds, but heat-treatment is detrimental to the surface –SOH sites important to the sorption of  $\text{Sr}^{2+}$ .

The study concluded that red muds, along with other metallurgical solid wastes and clay minerals, may be utilized for constructing natural barriers around shallow-land burial sites of low-level radioactive wastes and heavy metal-containing products (Apak et al. 1995).



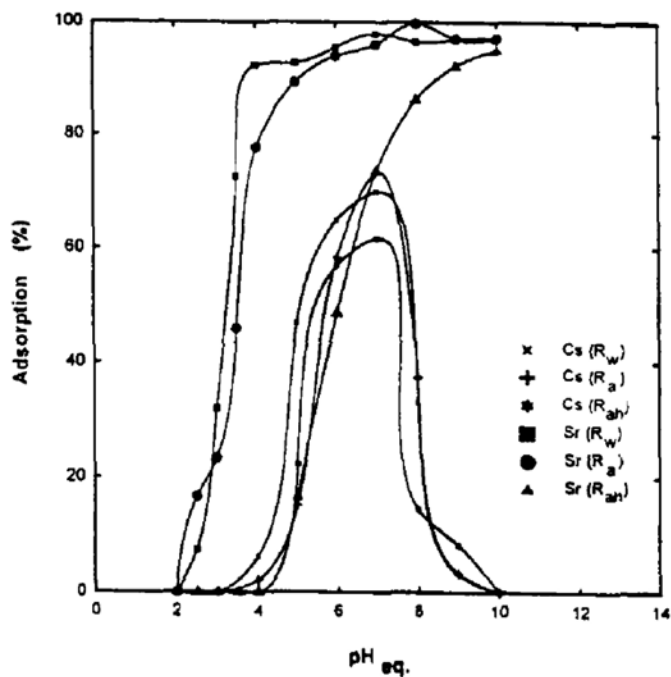


**Figure 5-7.** Graph of results from experiments investigating adsorption efficiency of  $\text{Cs}^+$  and  $\text{Sr}^{2+}$  to red mud treated with water, acid, or acid and heat as a function of pH (Apak et al. 1995).

**Table 5-8.** Chemical composition of a red mud studied for application in a low-level waste repository and results from  $\text{Cs}^+$  and  $\text{Sr}^{2+}$  adsorption experiments (Apak et al. 1995).

Red Mud (Applied to Nuclear Waste)	Apak et al. (1995)					
Chemical composition	wt%					
$\text{Fe}_2\text{O}_3$	37.26					
$\text{Al}_2\text{O}_3$	17.58					
$\text{SiO}_2$	16.94					
$\text{TiO}_2$	5.55					
$\text{Na}_2\text{O}$	8.31					
$\text{CaO}$	4.38					
Loss on ignition	7.17					
	97.19					
Treatment	RMwater		RMacid		RMacid+heat	
SBET ( $\text{m}^2/\text{g}$ )	14,2		20,7		28,0	
Lanmguir parameters	$\text{Cs}^+$	$\text{Sr}^{2+}$	$\text{Cs}^+$	$\text{Sr}^{2+}$	$\text{Cs}^+$	$\text{Sr}^{2+}$
Linearized eqn: $[(\text{Ai}-\text{Af})\text{V}/\text{m}]-1 = \text{sAf}-1 + \text{i}$						
$\text{Ai}, \text{f}$ = initial, final conc. In $\text{Bq}/\text{cm}^3$						
$\text{s}$ = slope	$6.97 \times 10^{-3}$	$6.93 \times 10^{-5}$	$5.59 \times 10^{-3}$	$1.36 \times 10^{-4}$	$2.71 \times 10^{-3}$	$1.13 \times 10^{-3}$
$\text{i}$ = intercept	$-2.40 \times 10^{-6}$	$1.8 \times 10^{-7}$	$-1.43 \times 10^{-6}$	$1.70 \times 10^{-7}$	$-3.4 \times 10^{-6}$	$5.19 \times 10^{-7}$
$\text{r}$ = correlation coefficient	0,959	0,965	0,989	0,957	0,983	0,986
Adsorption capacity in neutral solution ( $\text{mmol}/\text{g}$ )	$5.1 \times 10^{-3}$	10,6	$8.1 \times 10^{-3}$	12,5	$5.5 \times 10^{-2}$	5,9

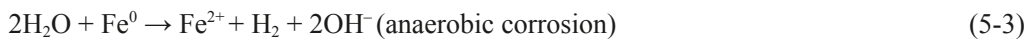
## 5.7 Zero-valent iron (ZVI) and corrosion products

Various studies have documented the ability of iron-based technologies to remediate contaminated soil and groundwater (Hashim et al. 2011), many of which focus on the remediation of arsenic contamination. They have also been investigated for application in deep geological repositories as canisters for the disposal of spent nuclear fuel (Kim et al. 2012). The redox and solubility behaviour of Fe as a function of Eh and pH is complex because it interacts with other metal ions through chemical, adsorption, and redox mechanisms. Oxidation state properties may have an important role in ion speciation and transport, especially in reducing environments. A redox-active surface may directly induce simple solution redox reactions (involving the transfer of electrons from one species to another), or a mineral surface may preferentially adsorb metal ions (Antonio and Soderholm 2006).

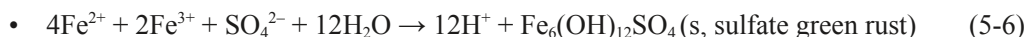
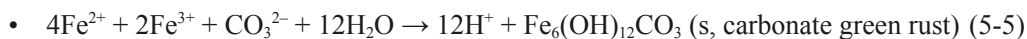
The survey found no studies to conclusively support the application of ZVI as an adsorbent in pure Fe<sup>0</sup> form. Where ZVI was classified as an adsorbent, the reactions occurring were actually in the order of species reduction by ZVI followed by sorption onto the particles formed by the Fe<sup>2+</sup> and Fe<sup>3+</sup> corrosion products. For example, Mamindy-Pajany et al. (2011) present data that suggests that As(V) is sorbing to the surface of ZVI, but they later conclude that arsenate adsorption onto ZVI is promoted when the oxidation of iron particles increases the number of active surface sites.

As applied to groundwater remediation, ZVI has been found to be a strong chemical reductant, with the ability to convert many mobile oxidized oxyanions (e.g. CrO<sub>4</sub><sup>2-</sup>, TcO<sub>4</sub><sup>-</sup>, MoO<sub>4</sub><sup>2-</sup>, AsO<sub>4</sub><sup>3-</sup>, and SeO<sub>4</sub><sup>2-</sup>) and oxyocations (e.g. UO<sub>2</sub><sup>2+</sup>) into immobile forms. Cantrell et al. (1995) studied the capability and rate at which Fe<sup>0</sup> removes CrO<sub>4</sub><sup>2-</sup>, TcO<sub>4</sub><sup>-</sup>, MoO<sub>4</sub><sup>2-</sup>, and UO<sub>2</sub><sup>2+</sup> from groundwater in order to determine the appropriate thickness of a permeable reactive barrier for remediation. It was found that the reduction of MoO<sub>4</sub><sup>2-</sup> to Mo<sup>3+</sup> by Fe<sup>0</sup> is thermodynamically favourable but to lesser extent than that of CrO<sub>4</sub><sup>2-</sup>. Also, the rate of MoO<sub>4</sub><sup>2-</sup> removal from solution was much slower than the other ions tested. Since experimental thermodynamic data involving the reduced forms of Mo were incomplete, it was assumed that the MoO<sub>4</sub><sup>2-</sup> was reduced to Mo<sup>3+</sup> which precipitated as a sparingly soluble Mo(OH)<sub>3</sub> (s). In a study investigating the effects of As and Mo in Se(VI) removal from drainage waters, Zhang et al. (2005) suggested three reasons for which an increase in Mo(VI) concentration may have reduced Se(VI) removal from a solution by Fe<sup>0</sup>. These relate to the redox, precipitation, and adsorptive processes that may occur between ZVI and MoO<sub>4</sub><sup>2-</sup>, removing the dissolved Mo from the solution. The first is that Mo(VI) is removed from solution when ZVI reduces it to Mo<sup>3+</sup>, which is incorporated into a Mo(OH)<sub>3</sub> precipitate. The second is that Mo(VI) oxyanions are adsorbed to iron hydroxide precipitates formed from the ZVI corrosion products. The third is that the Fe<sup>2+</sup> product of ZVI oxidation bonds with MoO<sub>4</sub><sup>2-</sup> to form Mo-Fe minerals, such as ferrous molybdate (FeMoO<sub>4</sub>).

Since a large number of species will be present and mobilized upon dissolution of the SFL wastes, the Eh, reflecting the overall redox potential of the repository environment, should be considered rather than interactions between ZVI, Fe<sup>2+</sup>, and Fe<sup>3+</sup> and a sole contaminant species in determining the system's oxidation states, species, and thus contaminant mobility. Regardless, iron corrodes under anoxic deep groundwater conditions by the reaction:



Green rust, or, fougérite, found as mineral in nature, is a type of LDH (see Section 5.4) that contains only Fe, but in both the 2+ and 3+ states, as cations in the brucite-type layers (Ruby et al. 2010). It is capable of intercalating anions, such as Cl<sup>-</sup>, CO<sub>3</sub><sup>2-</sup>, SO<sub>4</sub><sup>2-</sup>, etc to form chloride, carbonate, or sulfate green rusts, respectively, through the reactions:



Green rusts are well-known to adsorb oxyanions, such as phosphate, arsenate, and selenate (Jönsson and Sherman 2008 and references therein).

Synthetic carbonate green rust transforms spontaneously to magnetite and siderite, even under anaerobic conditions (Jönsson and Sherman 2008 and references therein). The sequence of iron corrosion is  $\text{Fe}(0) \rightarrow \text{FeCO}_3$  (siderite)  $\rightarrow (\text{Fe}_4^{\text{II}}\text{Fe}^{\text{III}}(\text{OH})_{12}\text{CO}_3)$  (green rust)  $\rightarrow \text{Fe}_3\text{O}_4$  (magnetite)  $\rightarrow \text{Fe}_2\text{O}_3$  (hematite) (Cui et al. 2009). Many studies have investigated the adsorption capacity of magnetite for different elements. Martínez et al. (2006) studied the sorption of selenium(IV) and selenium(VI) onto magnetite as a function of concentration and as a function of pH. At pH = 2, ~60% of the  $\text{SeO}_3^{2-}$  sorbed to 0.1 g of magnetite from a solution whose initial concentration was  $2 \times 10^{-5} \text{ mol dm}^{-3} \text{ SeO}_3^{2-}$ . This dropped to <5% at pH = 12. The results  $\text{SeO}_4^{2-}$  were ~10% sorbed at pH = 2 and <1% at pH = 12 (0.1 g of magnetite and  $[\text{Se}]_0 = 2 \times 10^{-5} \text{ mol dm}^{-3} \text{ SeO}_4^{2-}$ ). The sorption mechanism was surface complexation, inner-sphere complexation occurring with  $\text{SeO}_3^{2-}$  and outer-sphere with  $\text{SeO}_4^{2-}$ . Kim et al. (2012) studied the influence of carbonate and silicate anions on the sorption of selenium ions to magnetite and found that their competition hinders the sorption of selenite and selenate. This may have important implications if a vitrified waste form and a concrete barrier material are selected.

Many of the studies on selenium ion sorption and iron corrosion that have been discussed were undertaken in order to understand their behaviours in a deep geological repository for spent nuclear fuel. This application will differ from the SFL in terms of the critical nuclides, temperature, and engineered barrier materials. Such may have implications on the iron minerals expected to form during ZVI corrosion and this material will need more extensive modelling in order to draw useful adsorption efficiency inferences.

## 6 Discussion

As discussed in Section 3-1, the materials assumed in the concept analyzed in the preliminary safety assessment of the SFL 3-5 (SKB 1999) included steel, carbon steel, concrete, and gravel. Bedrock would also be expected to retard nuclide transport. The nuclide release rates and time of maximum release from both the near and the far field is dependent on the chemical characteristics of the nuclides and on site conditions, such as concentration of ions in the groundwater, Eh, and pH. Table 6-1 shows the groundwater components, Eh, and pH at each of the sites described in Section 3-1. The water at Aberg is saline and has high concentrations of Na<sup>+</sup> (2,100 mg/l), Ca<sup>2+</sup> (1,890 mg/l) SO<sub>4</sub><sup>2-</sup> (560 mg/l), and Cl<sup>-</sup> (6,410 mg/l). While pH is between 7 at Beberg 1 and 9.3 at Ceberg, the leached alkali hydroxides would have caused the pH of the cement pore water to initially be high (13.5). The pH would decrease as the portlandite (calcium hydroxide, Ca(OH)<sub>2</sub>) leached, being around pH 10 when only gel remained. As discussed in Section 3.1, such factors would have important effects on ion exchange and surface complexation processes.

Regarding the repository temperature, the preliminary safety assessment of the SFL 3-5 concept in 1999 (SKB 1999) assumed that temperature increases due to radioactive decay of the waste will not exceed 5°C during the first 100 years. This minor increase in temperature was assumed to influence neither processes of importance for the performance of the near-field barriers nor transport processes in the far-field. Temperatures at depths of 500 m for the sites considered in the reference scenario range from an average of 10.9°C to 14.6°C (SKB 1999). The temperatures at which adsorption experiments described in the literature were conducted, where stated, were largely between 20 and 30°C (Hashim et al. 2011, Mamindy-Pajany et al. 2011, Castaldi et al. 2010a, b, Goh et al. 2008). Temperatures prevailing in the near-field at the SFL are expected to be near the ambient temperature of most adsorption experiments. Crawford (2010) analyzed and recommended sorption partitioning data for use in the SR-Site safety assessment. Considering the uncertainties associated with the current adsorption processes and reactions, the conclusion was that the effect of temperature is expected to be small relative to the overall uncertainty of the sorption data, and it was neglected in the sorption calculations for the SR-Site (Crawford 2010).

**Table 6-1. Groundwater components, Eh, and pH at the sites used as input scenarios in the preliminary safety assessment of the SFL 3-5 (SKB 1999).**

Groundwater components	Unit	Aberg	Beberg 1	Beberg 2	Ceberg
Na <sup>+</sup>	mg/l	2,100	1,700	275	105
K <sup>+</sup>	mg/l	8	13	2	2
Ca <sup>2+</sup>	mg/l	1,890	1,650	142	21
Mg <sup>2+</sup>	mg/l	42	110	17	1
Sr <sup>2+</sup>	mg/l	35	21	—	—
Fe <sup>2+</sup>	mg/l	0.24	—	1.80	0.05
Mn <sup>2+</sup>	mg/l	0.29	0.82	0.13	0.01
HCO <sub>3</sub> <sup>-</sup>	mg/l	10	47	278	18
SO <sub>4</sub> <sup>2-</sup>	mg/l	560	370	49	0.1
Cl <sup>-</sup>	mg/l	6,410	5,500	555	178
I <sup>-</sup>	mg/l	—	0.12	—	0.14
Br <sup>-</sup>	mg/l	40	32	—	—
F <sup>-</sup>	mg/l	1.5	1.2	1.5	3.2
HS <sup>-</sup>	mg/l	0.15	< 0.01	—	< 0.01
NH <sub>4</sub> <sup>+</sup> calculated as N	mg/l	0.03	0.35	0.09	0.01
NO <sub>3</sub> <sup>-</sup> calculated as N	mg/l	< 0.010	< 0.005	< 0.002	0.009
NO <sub>2</sub> <sup>-</sup> calculated as N	mg/l	< 0.001	0.005	0.010	< 0.001
PO <sub>4</sub> <sub>tot</sub> calculated as P	mg/l	0.005	0.005	0.040	0.008
SiO <sub>2</sub> calculated as Si	mg/l	4.1	5.4	5.6	4.7
DOC (dissolved organic carbon)	mg/l	1	—	6	2
Eh	mV	-308	—	-250	-202
pH		7.7	7.0	7.9	9.3

Bentonite and zeolites are the most efficient cation exchangers. The bentonite that will be used in the SKB final repository for spent fuel has a capacity of  $\sim 1$  Eq/kg (Kamland, 2010), while that of the discussed zeolite varieties range between  $\sim 2.5$  and 5 Eq/kg. While bentonite has been extensively studied for spent fuel repository applications, it was not included as a barrier in the 1999 analysis. Like bentonite clay, some zeolites are very good cation exchangers. Many varieties of zeolites exist, each having a unique combination of mineralogical composition, framework structure, and cation exchange capacity. With respect to radioactive waste repository applications, the nuclide sorption potential has been investigated at sites where they may form as a result of concrete degradation and bedrock composition. Zeolite sorption properties have also been studied at repository sites where they occur naturally, such as at Yucca Mountain. Unlike the anion exchangers which, in general, function optimally at low pHs, zeolites form in alkaline and degrade in acidic conditions. However, efforts to optimize their application as cation exchangers for radionuclides in waste repositories have not been as direct as that of bentonite. In saline environments, competition among cations would be expected. At Aberg and Beberg 1, concentrations of  $\text{Na}^+$  and  $\text{Mg}^{2+}$  are relatively high, and these background ions could compete with cationic radionuclides for exchange sites. In some of the discussed zeolites,  $\text{Na}^+$  competes with cationic radionuclides. While  $\text{Cs}^+$  is consistently selected before  $\text{Na}^+$  and  $\text{Mg}^{2+}$  for exchange in the discussed zeolite varieties, its dose rate is high in only the near field of the SFL 3. Also important to note is that the matrix diffusion of anions into the bedrock is higher in saline water, so Cl-36, C-14, Mo-93 release rates in the far field are reduced at sites with long advective travel times and high flow-wetted surface areas. Thus, whereas the cation exchange efficiency could be high if zeolites were employed in a non-saline environment, the exchange efficiency of cationic radionuclides may be lower in saline environments due to the competitive effects of  $\text{Na}^+$ . Another issue may be the possibility for cation sieving to occur, especially since the wastes are comprised of a very large and diverse array of ions. While a zeolite may efficiently exchange a particular nuclide, the nuclides that remain may clog and damage the framework structure, thus reducing the cation exchange efficiency. To select a suitable zeolite for application in the SFL could be a long and tedious process. Moreover, cation adsorption to gravel and bedrock appears to sufficiently reduce the dose rates from cations in the near and far field. Bentonite and zeolites are not distinguished anion exchangers or adsorbents, and thus their application would probably fail to reduce the dose rates from anions such as I-129, Cl-36, C-14, and Mo-93.

Amphoteric adsorbents, such as metal oxides and hydroxides, adsorb both anions and cations through surface complexation reactions. Where the pH is below the  $\text{pH}_{\text{pzc}}$ , anions will be adsorbed, while where above the  $\text{pH}_{\text{pzc}}$ , cations will be adsorbed. An amphoteric material could be selected based on its  $\text{pH}_{\text{pzc}}$ . Therefore, if anion adsorption were desired, a metal oxide with a high  $\text{pH}_{\text{pzc}}$  would be preferred, particularly in an alkaline environment.  $\text{ZrO}_2$  and  $\text{ThO}_2$  have been found to have relatively high  $\text{pH}_{\text{pzc}}$ ,  $\sim \text{pH } 10$ . Still, their anion exchange capacities are  $< 0.25$  meq at this pH, and their application may have negligible dose release rates reduction effects.

Layered double hydroxides show the greatest potential as an anion exchanging material. Many classes of LDHs exist and have been investigated for environmental remediation applications. These vary by chemical composition, and in turn, by adsorption efficiency and selectivity series. They have not been studied for application in a radioactive waste repository, so it would be important to understand how the LDH would respond in a highly chemically complex system. The pH effect on the oxyanion adsorption depends on the type of oxyanion and the type of LDH. LDHs also have a  $\text{pH}_{\text{pzc}}$ , below which anions are adsorbed and above which  $\text{OH}^-$  may compete with other anions for sorption sites. Thus, concrete degradation may have negative effects on sorption efficiency. Since each class of LDH has a distinct selectivity series and LDHs are easy to fabricate, an important question would be whether one that selects for  $\text{MoO}_4^{2-}$ ,  $\text{Cl}^-$ ,  $\text{CO}_3^{2-}/\text{HCO}_3^-$ , and/or  $\text{I}^-$  could be designed and fabricated. If a saline environment is selected, the concentration of  $\text{Cl}^-$  in the water will be relatively high, and concrete degradation will release  $\text{CO}_3^{2-}/\text{HCO}_3^-$  and  $\text{OH}^-$  ions. Thus, another question would be whether these anions would interfere with the adsorption of radioactive anions. Or, could the intercalation of  $\text{Cl}^-$ ,  $\text{CO}_3^{2-}/\text{HCO}_3^-$  and  $\text{OH}^-$  from the intruding water and concrete dissolution products create a less permeable shield from the LDH particles?

Red mud is comprised of both the zeolite-like cation-adsorbing cancrinite and sodalite minerals and the amphoteric metal oxides, which can produce anion-adsorbing LDHs when treated with seawater. The specific mineralogy of a red mud is complex and varies with origin of deposit. This fact that it is comprised of assorted minerals may imply that it will be more difficult to model in a quantitative safety assessment than the previously discussed materials. However, the mineralogical diversity alongside its availability may make it a versatile and potentially economically viable adsorbent. Versatility could be an attractive trait, considering the inherent uncertainties under which this SFL concept development project currently operates. If untreated red mud could be utilized despite its high alkalinity, the cancrinite and sodalite minerals could exchange  $\text{Cs}^+$  and  $\text{Sr}^{2+}$  and other cations while the hydrous oxides could adsorb either cations or anions, depending on the overall  $\text{pH}_{\text{pzc}}$  of the red mud under consideration. If SFL is located in a saline environment, hydrotalcite could be produced upon interaction with seawater and adsorb anions. Or, the hydrotalcite produced from seawater-treated red mud could be placed in a non-saline environment and adsorb anions. This could dually enable a higher adsorption of Ni and other cationic radionuclide complexes to crushed rock or gravel and the bedrock. While additional adsorption scenarios could probably be imagined, it should be noted that the recycling of red mud into building materials has also been studied. Its trace heavy metal and radioactive U and Th contents have been noted as concerns in such applications. Akinci and Artir (2008) investigated the activity of the radium, uranium, thorium, and potassium from the red mud of the ETI Seydisehir Aluminum Plant. It was determined that the activity safety limit value of the red mud satisfied the regulations of EU safety limits for radioactivity in materials which are not frequently in direct contact with human workers, such as bricks and roof tiles. If the concrete barrier functions only to package the wastes and to induce alkaline conditions, then it may be possible to replace the cement envisioned in the 1999 PSA reference design with red mud cement. Currently, low-Al varieties are preferred in the ordinary Portland cement due to the concern that ettringite or Friedel's salt will form if sulphate or chloride, respectively, in the water reacts with calcium aluminate minerals. Although these products may lead to cracking, ettringite may substitute anions into its structure during formation and has a positively charged surface that can lead to further ion removal through adsorption (Zhang and Reardon 2003).

The direct sorption efficiency of zero-valent iron is probably less advantageous than the previously discussed materials. Still, ZVI may suit the retardation/slow-release concept because it is a powerful reductant that, upon its own oxidation, may form minerals that could adsorb or incorporate the released nuclides. At this juncture, one cannot infer which nuclides would be reduced to immobile forms, adsorbed to Fe-minerals, or precipitated as Fe-minerals. Since hematite is the final corrosion product of ZVI and is a significant constituent of red mud, further work should focus on its sorption properties in any further consideration of these materials.

While the nuclide speciation and the mineralogical composition of the material will have a significant impact on the adsorption processes and efficiency, the literature that this report relies on was found to be too general to draw conclusions specific to the SFL wastes and repository, particularly at this stage in the concept development process when the waste-form is yet undetermined. Thus, this report can only assume the speciation of the nuclides in the presumed conditions and offer broad trends regarding the redox states and processes. Further investigation into the preferred material(s) should aim to develop more specific data with regards to the redox variables.

The materials discussed, particularly those comprised of oxide minerals, may tend to form colloids, making the electrophoretic mobility an important parameter for consideration in future investigations. This will be dependent on the zeta potential of the colloidal oxide particles themselves and the ionic strength of the groundwater. A saline environment will tend to promote the coagulation or flocculation of the particles, thus reducing their dispersal, while dually promoting the diffusion of anions into the rock matrix (matrix diffusion, noted in Section 3.1). While these factors may reduce release rate, ions in the groundwater may compete for adsorption sites. Thus, future work should be focused towards understanding the broader adsorption trends as extrapolated from experimental results.



## 7 Conclusions

Certain bentonite and zeolite varieties are very efficient cations exchangers, and their performance as such would not be hindered in the neutral to alkaline pH conditions likely to be relevant to the selected site. However, results from the 1999 preliminary safety assessment of the SFL 3-5 concept suggest that that dose rates from cations will be low relative to those from anions in each scenario analyzed. If cation migration increases due to decreased adsorption to concrete, gravel, or bedrock or to the selection of a site with saline conditions, then the barrier potential of bentonite and/or zeolites may be investigated further. In such, it should be noted that the heterogeneity of chemical complexes in this system may induce cation-sieving effects and reduce the exchange efficiency of the zeolite. A zeolite with both a high CEC and large channels (through which the larger nuclide complexes can flow freely) may exist. Yet, considering the substantial number of zeolite varieties and the associated diversity in chemical and structural properties, to select and develop such for this application may prove a tedious and resource-intensive process. Since these sieving effects would not be expected to occur in bentonite and since it has been extensively studied for long-term nuclear waste repository application, bentonite may be a more attractive material for the adsorption of cations. Still, the overall repository concept must be considered to validate this notion.

The application of additional cation exchange materials will not obviate the need for a reduction in the dose rates expected to result from the release of anions. Hydrous metal oxides and LDHs are the most notable anion exchangers, considering the requirements for application as a barrier material for the long-term. However, the expected reduced performance in an alkaline environment is a major obstacle to their utilization. Still, their availability is potentially substantial if untreated or treated red mud could be a source. In addition to containing metal oxide, LDH, and zeolite-like minerals, it has also been investigated for application as cement or as a brick-like building material.

Iron in the zero-valent state is not a confirmed or significant adsorbent, and in anoxic conditions it will corrode, possibly to fougurite first and then to hematite. This process would simultaneously release electrons that would keep some nuclides in reduced and insoluble forms. Still, deep groundwater conditions are commonly already reducing, and application of ZVI for such function may be redundant. Fougurite (or, green rust), can intercalate anions. However, the specific anions and the respective adsorption efficiencies would require further investigation. Moreover, the  $\text{Fe}^{2+}$  in the fougurite will eventually corrode and result in hematite. This process may release some of the ions adsorbed to the fougurite, but hematite itself may have relevant sorption properties. The ZVI corrosion chain, alongside the high red mud hematite contents, may warrant further investigation into its sorptive properties.

Red mud appears to be the most versatile material, and it is potentially available in substantial quantities. Further survey may compare its sorptive properties, costs, and integrity as a building material to those of Portland cement and its concretes. Yet, as further siting, design, and budgeting decisions are made, future analyses should heed the fact that each material has sorptive and/or economic advantages and disadvantages.

## References

SKB's (Svensk Kärnbränslehantering AB) publications can be found at [www.skb.se/publications](http://www.skb.se/publications).

- Akinci A, Artir R, 2008.** Characterization of trace elements and radionuclides and their risk assessment in red mud. *Materials Characterization* 59, 417–421.
- Amphlett C B, McDonald L A, Redman M J, 1958.** Synthetic inorganic ion-exchange materials – II: Hydrous zirconium oxide and other oxides. *Journal of Inorganic and Nuclear Chemistry* 6, 236–245.
- Antonio M R, Soderholm L, 2006.** X-ray absorption spectroscopy of the actinides. In Morss L R, Edelstein N M, Fuger J (eds). *The chemistry of the actinide and transactinide elements*. Dordrecht: Springer, 3086–3198.
- Apak R, Atun G, Güclü K, Tütem E, Keskin G, 1995.** Sorptive removal of cesium-137 and strontium-90 from water by unconventional sorbents. I. Usage of bauxite wastes (red muds). *Journal of Nuclear Science and Technology* 32, 1008–1017.
- Bradbury M H, Baeyens B, 2011.** Physico-chemical characterisation data and sorption measurements of Cs, Ni, Eu, Th, U, Cl, I and Se on MX-80 Bentonite. Nagra Technical Report 09-08, National Cooperative for the Disposal of Radioactive Waste, Switzerland.
- Bradbury M H, Baeyens B, Thoenen T, 2010.** Sorption data bases for generic Swiss argillaceous, crystalline and calcareous rock systems. PSI-Bericht 10-03, Paul Scherrer Institut, Switzerland.
- Breck D W, 1974.** Zeolite molecular sieves: structure, chemistry and use. New York: Wiley.
- Cantrell K J, Kaplan D I, Wietsma T W, 1995.** Zero-valent iron for the in situ remediation of selected metals in groundwater. *Journal of Hazardous Materials* 42, 201–212.
- Castaldi P, Silvetti M, Enzo S, Melis P, 2010a.** Study of sorption processes and FT-IR analysis of arsenate sorbed onto red muds (a bauxite ore processing waste). *Journal of Hazardous Materials* 175, 172–178.
- Castaldi P, Silvetti M, Garau G, Deiana S, 2010b.** Influence of the pH on the accumulation of phosphate by red mud (a bauxite ore processing waste). *Journal of Hazardous Materials* 182, 266–272.
- Chapman N, Apted M, Glasser F, Kessler J, Voss C, 2000.** Djupförvar för långlivat låg- och medelaktivt avfall i Sverige (SFL 3-5). En internationell expertgranskning av SKB:s preliminära säkerhetsanalys. SKI Rapport 00:54, Statens kärnkraftinspektion (Swedish Nuclear Power Inspectorate). (In Swedish.)
- Conca J, Strietelmeier E, Lu N, Ware S S, Taylor T P, Kaszuba J, Wright J, 2002.** Treatability study of reactive materials to remediate ground water contaminated with radionuclides, metals, and nitrates in a four-component permeable reactive barrier. In Naftz D L, Morrison S J, Davis J A, Fuller CC (eds). *Handbook of groundwater remediation using permeable reactive barriers: applications to radionuclides, trace metals and nutrients*. San Diego, CA: Academic Press, 221–252.
- Cornell R M, Schwertmann U, 2003.** The iron oxides: structure, properties, reactions occurrences, and uses. 2nd ed. Weinheim: Wiley-VCH.
- Crawford J, 2010.** Bedrock  $K_d$  data and uncertainty assessment for application in SR-Site geosphere transport calculations. SKB R-10-48, Svensk Kärnbränslehantering AB.
- Cui D, Puranen A, Devoy J, Scheidegger A, Leupin O X, Wersin P, Gens R, Spahiu K, 2009.** Reductive immobilization of  $^{79}\text{Se}$  by iron canister under simulated repository environment. *Journal of Radioanalytical and Nuclear Chemistry* 282, 349–354.
- Davis J A, Kent D B, 1990.** Surface complexation modeling in aqueous geochemistry. In Hochella M F, White A F (eds). *Mineral-water interface geochemistry*. Washington, DC: Mineralogical Society of America, 177–260 journal.
- Dyer A, 2000.** Ion exchange. In Wilson I D (ed). *Encyclopedia of separation science*. San Diego, CA: Academic Press, 156–173.



- Eby G N, 2004.** Principles of environmental geochemistry. Pacific Grove, CA: Thomson-Brooks/Cole.
- Geological Survey of Japan, 2005.** Atlas of Eh-pH diagrams: intercomparison of thermodynamic databases. Open file report 419, Geological Survey of Japan. Available at: <http://www.gsj.jp/GDB/openfile/files/no0419/openfile419e.pdf> [9 July 2012].
- Goh K-H, Lim T-T, Dong Z, 2008.** Application of layered double hydroxides for removal of oxyanions: a review. *Water Research* 42, 1343–1368.
- Gottardi G, 1978.** Mineralogy and crystal chemistry of zeolites. In Sand L B, Mumpton F A (eds). *Natural zeolites: occurrence, properties, use*. Oxford: Pergamon, 31–44.
- Hashim M A, Mukhopadhyay S, Sahu J N, Sengupta B, 2011.** Remediation technologies for heavy metal contaminated groundwater. *Journal of Environmental Management* 92, 2355–2388.
- Jeppu G P, Clement T P, 2012.** A modified Langmuir-Freundlich isotherm model for simulating pH-dependent adsorption effects. *Journal of Contaminant Hydrology* 129–130, 46–53.
- Jönsson J, Sherman D M, 2008.** Sorption of As(III) and As(V) to siderite, green rust (fougerite) and magnetite: implications for arsenic release in anoxic groundwaters. *Chemical Geology* 255, 173–181.
- Kang M J, Rhee S W, Moon H, Neck V, Fanghanel T, 1996.** Sorption of  $\text{MO}_4^-$  (M = Tc, Re) on Mg/Al layered double hydroxide by anion exchange. *Radiochimica Acta* 75, 169–173.
- Kang M J, Chun K S, Rhee S W, Do Y, 1999.** Comparison of sorption behavior of  $\text{I}^-$  and  $\text{TcO}_4^-$  on Mg/Al layered double hydroxide. *Radiochimica Acta* 85, 57–63.
- Karnland O, 2010.** Chemical and mineralogical characterization of the bentonite buffer for the acceptance control procedure in a KBS-3 repository. SKB TR-10-60, Svensk Kärnbränslehantering AB.
- Kim S S, Min J H, Lee J K, Baik M H, Choi J-W, Shin H S, 2012.** Effects of pH and anions on the sorption of selenium ions onto magnetite. *Journal of Environmental Radioactivity* 104, 1–6.
- Mamindy-Pajany Y, Hurel C, Marmier N, Romeo M, 2011.** Arsenic(V) adsorption from aqueous solution onto goethite, hematite, magnetite and zero-valent iron: effects of pH, concentration and reversibility. *Desalination* 281, 93–99.
- Martínez M, Giménez J, de Pablo J, Rovira M, Duro L, 2006.** Sorption of selenium(IV) and selenium(VI) onto magnetite. *Applied Surface Science* 252, 3767–3773.
- Mokaya R, 2000.** Novel layered materials: non-phosphates. In Wilson I D (ed). *Encyclopedia of separation science*. San Diego, CA: Academic Press, 1610–1617.
- Mumpton F A, 1999.** La roca magica: uses of natural zeolites in agriculture and industry. *Proceedings of the National Academy of Sciences* 96, 3463–3470.
- Palmer S J, Frost R L, Nguyen T M, 2009.** Hydrotalcites and their role in coordination of anions in Bayer liquors: anion binding in layered double hydroxides. *Coordination Chemistry Reviews* 253, 250–267.
- Palmer S J, Nothling M, Bakon K H, Frost R L, 2010.** Thermally activated seawater neutralised red mud used for the removal of arsenate, vanadate and molybdate from aqueous solutions. *Journal of Colloid and Interface Science* 342, 147–154.
- Parks G A, 1990.** Surface energy and adsorption at mineral-water interfaces: an introduction. In Hochella M F, White A F (eds). *Mineral-water interface geochemistry*. Washington, DC: Mineralogical Society of America, 133–175 journal.
- Ruby C, Usman M, Naille S, Hanna K, Carteret C, Mullet M, François M, Abdelmoula M, 2010.** Synthesis and transformation of iron-based layered double hydroxides. *Applied Clay Science* 48, 195–202.
- Sahai N, 2000.** Estimating sorption enthalpies and affinity sequences of monovalent electrolyte ions on oxide surfaces in aqueous solutions. *Geochimica et Cosmochimica Acta* 64, 3629–3641.
- Santona L, Castaldi P, Melis P, 2006.** Evaluation of the interaction mechanisms between red muds and heavy metals. *Journal of Hazardous Materials* 136, 324–329.

- Savage D, 2011.** A review of analogues of alkaline alteration with regards to long-term barrier performance. *Mineralogical Magazine* 75, 2401–2424.
- SKB, 1999.** Deep repository for long-lived low- and intermediate-level waste, preliminary safety assessment. SKB TR-99-28, Svensk Kärnbränslehantering AB.
- SKB, 2011.** Long-term safety for the final repository for spent nuclear fuel at Forsmark. Main report of the SR-Site project. Volume 1. SKB TR-11-01, Svensk Kärnbränslehantering AB.
- Tombácz E, 2002.** Adsorption from electrolyte solutions. In Tóth J (ed). *Adsorption: theory, modeling, and analysis*. New York: Marcel Dekker, 711–742.
- Toraishi T, Nagasaki S, Tanaka S, 2002.** Adsorption behavior of  $\text{IO}_3^-$  by  $\text{CO}_3^{2-}$ – and  $\text{NO}_3^-$  hydrotalcite. *Applied Clay Science* 22, 17–23.
- Treacy M M J, 2010.** Zeolite structure prediction and the identification of useful synthetic targets. Report 46779-AC10, American Chemical Society. Available at: <http://acswebcontent.acs.org/prfar/2009/reports/P10550.html>
- Wang Y, Gao H, 2006.** Compositional and structural control on anion sorption capability of layered double hydroxides (LDHs). *Journal of Colloid and Interface Science* 301, 19–26.
- Vaughan D E W, 1978.** Properties of natural zeolites. In Sand L B, Mumpton F A (eds). *Natural zeolites: occurrence, properties, use*. Oxford: Pergamon, 353–355.
- White D A, Rautiu R, 1997.** The sorption of anionic species on hydrous tin dioxide. *Chemical Engineering Journal* 66, 85–89.
- Wulfsberg G, 1987.** *Principles of descriptive inorganic chemistry*. Monterey, CA: Brooks/Cole Publishing Company.
- Zhang M, Reardon E J, 2003.** Removal of B, Cr, Mo, and Se from wastewater by incorporation into hydrocalumite and ettringite. *Environmental Science & Technology* 37, 2947–2952.
- Zhang Y, Amrhein C, Frankenberger W T, 2005.** Effect of arsenate and molybdate on removal of selenate from an aqueous solution by zero-valent iron. *Science of the Total Environment* 350, 1–11.